Synthesis of Amino Terminal Clicked dendrimers. Approaches to the application as a biomarker

Noemi Molina,[†,‡] Francisco Nájera,[†,‡] Juan A. Guadix,[#,‡] Jose M. Perez-Pomares,[#,‡] Yolanda Vida,[*, †,‡] and Ezequiel Perez-Inestrosa[*, †,‡]

[†] Departamento de Química Orgánica, Facultad de Ciencias, Universidad de Málaga - IBIMA, Campus de Teatinos s/n, 29071 Málaga, Spain

[‡] Centro Andaluz de Nanomedicina y Biotecnología (BIONAND), Junta de Andalucía, Universidad de Málaga, C/ Severo Ochoa 35, 29590 Campanillas (Málaga), Spain

[#] Departamento de Biología Animal, Facultad de Ciencias, Universidad de Málaga - IBIMA, Campus de Teatinos s/n, 29071 Málaga, Spain

KEYWORDS. Dendrons, Dendrimers, Click reactions, DOSY experiments and Molecular Dynamic Simulations.

ABSTRACT: Herein we present an easy and efficient synthesis of amino terminal dendrons combining protection/deprotection reactions with copper-catalyzed azide alkyne cycloaddition in a convergent way. This new approach affords dendrons in gram scale with excellent yields and easy purification. By choosing the appropriate azido functionalized core, those dendrons lead to more efficient and controlled convergent synthesis of dendrimers with different size, shape and multivalence. The amino terminal dendrimers were analyzed by Diffusion-Ordered Spectroscopy experiments. The observed dendrimer size is in excellent correlation with the expected size and shape by Molecular Dynamic Simulations. The construction of these kinds of nanostructures in a simple and efficient way, opens new opportunities for biomedical applications. Moreover, by choosing the appropriate core, this versatile macromolecules becomes an excellent fluorescent biomarker.

INTRODUCTION

The design and synthesis of improved biocompatible polymeric materials is an important topic nowadays due to their widespread use in biomedicine. In particular, dendrimers are excellent candidates for many biomedical applications, especially where linear homologs are not effective.[1] Dendrimers are highly branched macromolecules with an extremely orderly structure. Their synthetic procedures, based on a stepwise growth, afford well defined and monodisperse compounds. The structures of the core, branch multiplicities and branch segment length have a significant effect on the overall structure and properties of the dendrimer, defining the number and density of functional groups at the periphery, usually increasing exponentially with each generation. [2–5] These attributes, together with their synthetic versatility, make dendrimers excellent scaffolds for many biomedical applications.[1]

For biomedical purposes, nearly all dendrimers are modified by a conjugation of their terminal groups with at least one type of ligand. Amino terminal dendrimers are an excellent alternative, since this functional group reacts easily with a great number of bioactive molecules. Another important key for some bioapplications is stability, especially where the dendrimer plays the role of a carrier molecule, for example in emulating the carrier protein in the hapten-carrier conjugate involved in allergic reactions.[6–8]

The most suitable and available amino terminal dendrimers are Vögtle`s polypropylenimine (PPI),[9] Denkewalter`s poly(L-lysine) (PLL),[10] Tomalia`s polyamidoamine (PAMAM),[11,12] and more recently a modification proposed by Malkoch from Hult´s polyester (bis-MPA).[13] While these dendrimers are characterized by their symmetrical branching, PLL differs in their asymmetry.[14] Nevertheless, limitations regarding synthesis, quality or stability of those dendrimers have been reported. The most extended used is PAMAN, the first commercially-available even for high generations. However, the stability and quality of PAMAM dendrimers have been previously questioned.[15] Moreover, their synthesis requires long reaction times and large excess of monomers to reach full conversions. For instance, defects are reported to be present in their structure due to retro-Michael additions and intramolecular lactam formation.[1] Similarly, PPI dendrimer growth can be limited by retro-Michael reactions or intramolecular amine cyclization. It has been reported that for the fifth generation, only 29% of the dendrimer will be defect-free.[1] Another aspect to take into account for certain applications is the high basicity of PAMAM and PPI. The conformation of both dendrimers is strongly affected by low pH due to electrostatic repulsion of the protonated internal tertiary amines.[1] On the other hand, polyester (bis-MPA) dendrimers can be synthetized and purified more efficiently and also post-

functionalized to display terminal amino groups up to generation five.[13] However, the lack of stability due to the reported hydrolysis of the ester bond may be a problem for certain applications in which the steadiness of the dendrimer is required.[13]

We previously reported a new class of amino terminal dendrimer constructed through amide linkages. Using a divergent approach, this novel polyamide dendrimer (BAPAD) was synthetized based on a 3,3′-diaminopivalic acid scaffold.[16] Their excellent stability allowed the use of such dendrimers for different bioapplications.[17,18] However, despite the versatility of the system, the maximum generation of the amino terminal dendrimer obtained was generation 3, which contains 16 peripheral amino groups.[16,19] This could be explained by a dramatic decrease in the reactivity of the azide groups caused by a backfolding of these surface groups. This effect has been previously observed and is more pronounced when the synthesis of the dendrimer is performed in a divergent way.[19] All mentioned dendrimers were synthetized following a divergent approach, and chromatographic procedures were required in all cases. Although some of the purification procedures are well established, they are tedious and time consuming.

The convergent approach for dendrimer synthesis was introduced by Hawker and Fréchet.[20] This methodology proceeds from the surface of the dendrimer inward to form a dendron that reacts with a suitable core to complete the synthesis. The advantage of the convergent approach is that only a limited number of active sites are present in each reaction, reducing the structural defects of the product. However, this methodology is used to form relatively lower generation dendrimers because steric hindrance can make the coupling of large dendrons with small cores difficult.[21] To increase coupling yields for the convergent approach, the 1,3-dipolar cycloaddition reactions results an excellent candidate.[22] The copper-catalyzed azide-alkyne "click" cycloaddition (CuAAC) requires mild reaction conditions and simple work-up procedures, tolerates a wide range of functional groups, including aqueous media, and results in 1,4-regiospecific 1,2,3-triazole formation in high yields.[23] All these features made Click chemistry an excellent tool in the construction of a large variety of dendritic structures with high level of efficiency, and have been used to improve traditionally synthetic processes.[24–27]

Herein we present a simple, convenient and efficient method for the synthesis of stable and water soluble amino terminal dendrimer taking advantage of Click reactions. Different generation dendrons have been prepared combining protection/deprotection reactions and copper-catalyzed azide alkyne cycloaddition, in a convergent way. To increase dendron generation, 3 synthetic steps are involved: click reaction, deprotection (hydrogenation) and amide formation. All reactions with already well stablished protocols, excellent yields (above 85%), easy purification procedures (no chromatography is needed), cheap reactants and carried out on a gram scale. The coupling of those alkyne-bearing dendrons to azide cores using click chemistry gives as a results different dendrimers in one step. The goal of this synthetic strategy relays in the versatility of the methodology. With a third generation dendron it is possible the construction of dendrimers with different size, shape or amount of amino terminal groups by choosing the appropriate core. By changing the multiplicity and functionality of the core, we can design and prepare stable amino terminal dendrimers with a specific ability, size or shape for a particular application. The easy and efficient synthesis of the dendrimer was carried out in one step, using click chemistry to couple alkyne-bearing dendrons to azide cores. The dendrimers were completely characterized and Diffusion-Ordered Spectroscopy (DOSY) experiments were used to determine the sizes and shape of the dendrimers. Results are in good agreement with calculated values. As a proof of concept, a fluorescent core was chosen to prepare a luminescent dendrimer whose abilities as biosensor has been proved, labeling bacteria cells with a characteristic fluorescence which can be used for two-photon excitation microscopy.

RESULTS AND DISCUSSION

Motivated by the efficiency and versatility of the copper-mediated click transformation, we designed a divergent synthetic route for new dendrons based on 3,3′-diazidopivalic acid as building block. The azide groups permit the growth of the dendrimers by CuAAC reactions. The final step in the dendrimer synthesis consists of the coupling between an alkyne functionalized dendron and an azido-bearing central core.

Synthesis of Dendrons

The propargyl-functionalized dendrons (**dGn**) were synthetized following the procedure shown in Scheme 1. 3,3′-diazidopivalic acid was prepared under previously described procedures.[16] The protection of the carboxylic acid function as benzylic ester gives as result the monomer used in the synthesis.

To obtain the first generation dendron (**dG1**, Scheme 1), azide groups were reduced. According to a convergent approach, these resulting groups will be placed on the surface of the final dendrimer. After protection of those amino groups and deprotection of the carboxylic acid, the compound was reacted with propargyl amine to yield **dG1** in excellent yields. From this point, the growth of dendrons involves three iterative steps: (i) "click" reaction between **dGn** and the monomer (ii) hydrogenation reaction for carboxylic acid deprotection and (iii) amide formation via propargyl amine reaction.

For the first step, a general procedure for the reaction between azides and alkynes was used. A mixture of azide, alkyne, $CuSO_4$ and sodium ascorbate in water/*tert*-butyl alcohol (2:1) was stirred at room temperature. The crude was recovered in CH_2Cl_2 and washed with an ammonia/brine mixture to eliminate the copper excess. The final products were precipitated with hexane to yield pure dendrons with more than 90% yields. A slight excess of the alkyne derivative with respect to the azide was used in order to ensure the reaction of all branches of the dendrons. These reactions were monitorized by IR and NMR spectroscopies.

Scheme 1. Synthesis of **dG1-dG3** dendrons

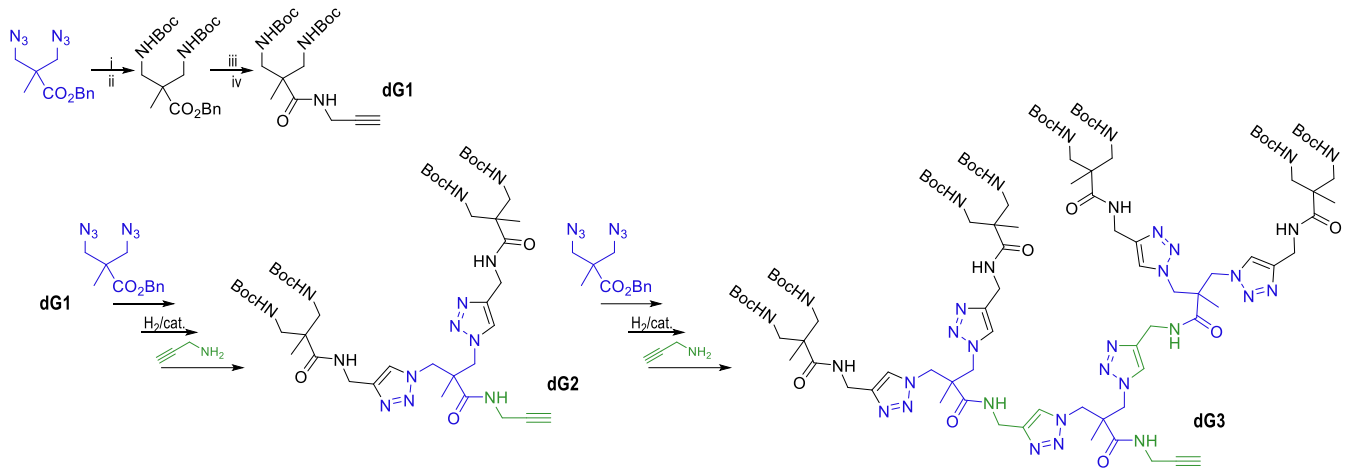

Reagents and conditions: i) 1) PPh_3, THF, 2) H_2O, 98%; ii) $(Boc)_2O$, acetone:H_2O, 96%; iii) H_2, $Pd(OH)_2$, MeOH, quantitative; iv) Propargylamine, CDI, CH_3CN, 83%.

The complete reaction of the azide moieties is confirmed by the IR spectra. Figure 1 (insets) shows the IR spectra of the resulting compounds of click reactions between benzyl-3,3′-diazidopivaloate with **dG1** (namely **dG2-CO_2Bn**) and **dG2** (namely **dG3-CO_2Bn**). The disappearance of the intense azide associated signal at 2085 cm^{-1} indicates in both cases the complete reaction of azide groups. The formation of the 1,2,3-triazole ring in clicked compounds was confirmed by their ^{1}H-NMR spectra, appearing new peaks between 7.7-8.0 ppm where triazole proton resonance peaks are observed (d and d′ in Figure 1). Additionally, in both cases the ^{1}H-NMR spectra indicate the complete reaction of the alkyne moiety, since the peak around 3.8 ppm, corresponding to the adjacent methylene (b for **dG1**, Figure 1a), are shifted to lower field (around 4.27 ppm, b and b′, Figure 1b and 1c). The hydrogenation reaction for carboxylic acid deprotection resulted quantitative for all cases. Finally, products obtained after reaction with propargyl amine were precipitated to yield pure dendrons with excellent yields. It should be noted that no chromatography is need for purification.

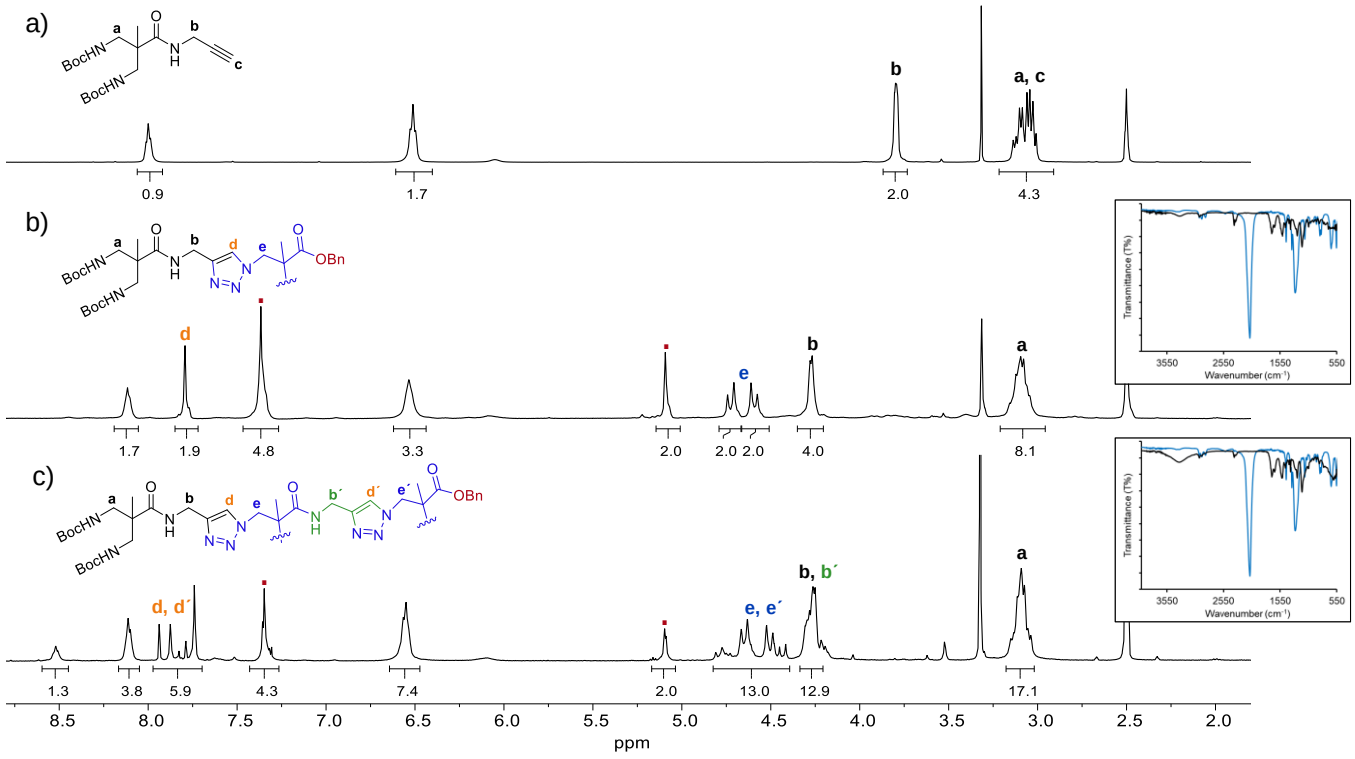

Figure 1. NMR spectra in DMSO-d_6 of a) **dG1**, b) **dG2-CO_2Bn** and c) **dG3-CO_2Bn**. Inset: b) IR spectra of benzyl-3,3′-diazidopivaloate (blue) and **dG2-CO_2Bn** (black) and c) IR spectra of benzyl-3,3′-diazidopivaloate (blue) and **dG3-CO_2Bn** (black)

Scheme 2. Synthesis of $\mathbf{Gn_{EDA}NH_2}$ dendrimers

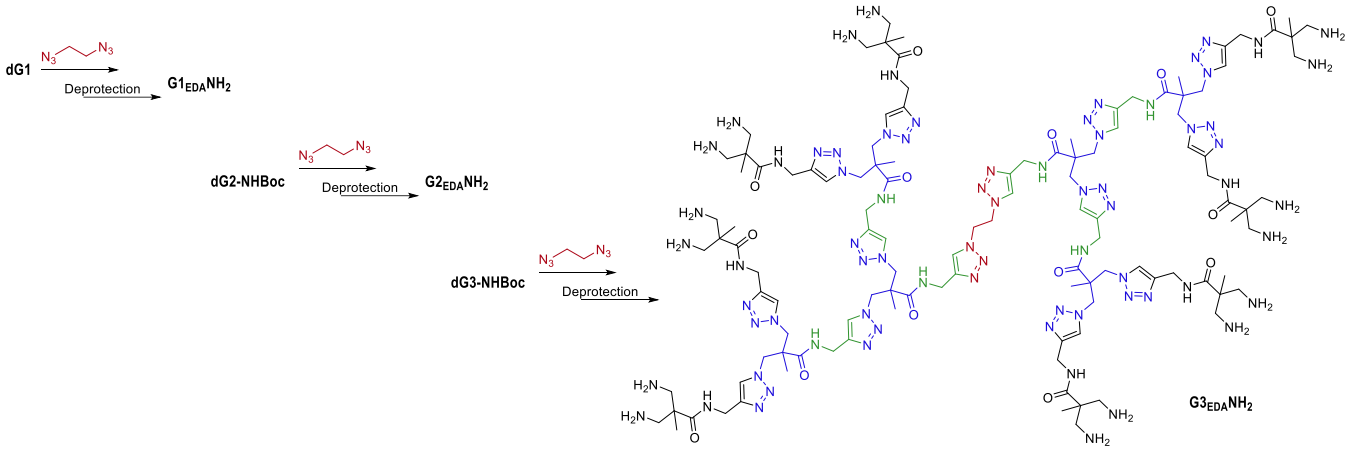

Reagents and conditions: $CuSO_4$, sodium ascorbate, water/*tert*-butyl alcohol (2:1) for click coupling; HCl 4M in dioxane, THF for amino deprotection.

Synthesis of Dendrimers

For an effective connection between the propargyl focal point of dendrons and azide-functionalized cores, alkane, aromatic and fluorescent moieties were designed in order to achieve dendrimers with different functionalities, size and number of terminal amino groups. In this sense 1,2-diazidoethane, 1,3,5-tris(azidomethyl)benzene and *N*-(3-azidopropyl)-4-((3-azidopropyl)amino)-1,8-naphthalimide were prepared. The efficiency of this methodology for the construction of different generation dendrimers were evaluated using 1,2-diazidoethane as core. This compound was prepared according to a previously reported procedure,[28] and coupled with generation 1 (**dG1**), 2 (**dG2**) and 3 (**dG3**) dendrons (Scheme 2).

Click reactions afford the corresponding dendrimers in excellent yields (92%, 80% and 93% for generations 1, 2 and 3). The deprotection reactions of the terminal amino groups were carried out under acidic conditions, yielding $\mathbf{G1_{EDA}NH_2}$, $\mathbf{G2_{EDA}NH_2}$ and $\mathbf{G3_{EDA}NH_2}$, respectively in an almost quantitative way for all cases (Scheme 2). The complete click reactions of alkyne dendrons with 1,2-diazidoethane to yield $\mathbf{G1_{EDA}NHBoc}$, $\mathbf{G2_{EDA}NHBoc}$ and $\mathbf{G3_{EDA}NHBoc}$ were confirmed by the IR spectra (inset, Figure 2).

The formation of two news 1,2,3-triazole rings in dendrimers was confirmed by ^{1}H-NMR (Figure 2) by the appearance of triazole proton, d′′ and the adjacent methylene, f in Figure 2. Additionally, the peaks around 3.8 ppm in **dG1**, **dG2** and **dG3** spectra corresponding to the adjacent methylenes of the alkyne moiety (Figures S11, S20 and S29, ESI, respectively), are shifted to lower field (around 4.27 ppm, b, b′ and b′′ in Figure 2) in dendrimers.

In a similar way, **dG3** was coupled to the other azido-cores yielding after amino deprotection $\mathbf{G3_{3AB}NH_2}$ and $\mathbf{G3_{Naph}NH_2}$ (Scheme 3). Tri-substituted benzene was chosen to introduce a rigid core in the molecule. A fluorescent naphthalimide moiety was selected in order to introduce a functional core in the molecule, since the potential applications of luminescent dendrimer are well known.[29] Tri-azidomethyl benzene was synthetized following previously described procedures.[30] *N*-(3-azidopropyl)-4-((3-azidopropyl)amino)-1,8-naphthalimide was prepared by coupling 3-azidopropylamine (obtained from 3-Bromopropylamine) with 4-bromo-1,8-naphthalic anhydride in DMSO, heating at 80ºC overnight.

Click reactions with **dG3** were carried out under the conditions described earlier, and the reactions were monitored in a similar way as for the previous dendrimers, in terms of the disappearance of the azide signal in IR (ensuring reaction of all branches of the core, Figures S78 and S79, ESI) and the generation of new signals in ^{1}H-NMR (Figures S52 and S62, ESI). Both dendrimers were obtained with good yields and deprotection reactions of the terminal amino groups yielded $\mathbf{G3_{3AB}NH_2}$ and $\mathbf{G3_{Naph}NH_2}$ in an almost quantitative way (Scheme 3).

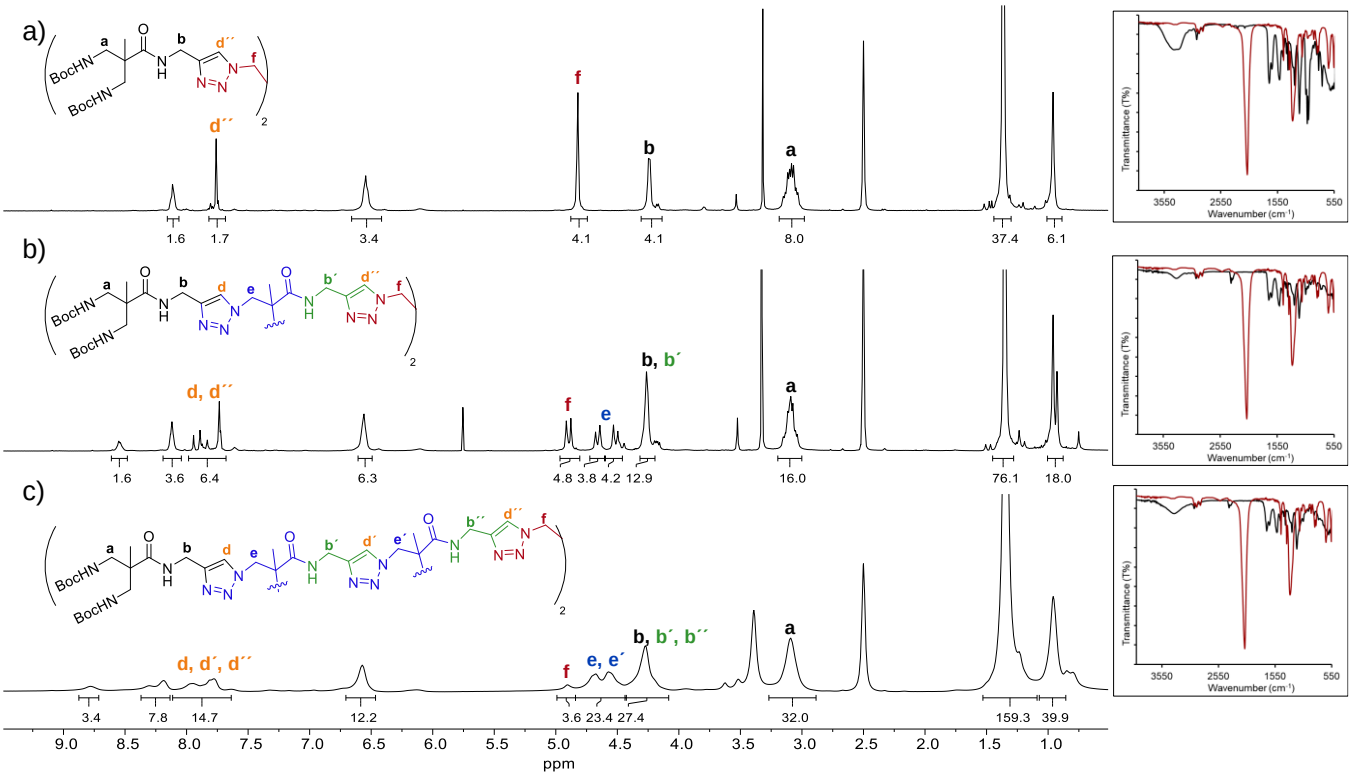

Figure 2. NMR spectra in DMSO-d$_6$ of a) **G1$_{EDA}$NHBoc**, b) **G2$_{EDA}$NHBoc** and c) **G3$_{EDA}$NHBoc**. Inset: IR spectra of 1,2-diazidoethane (red) and a) **G1$_{EDA}$NHBoc** (black), b) **G2$_{EDA}$NHBoc** and c) **G3$_{EDA}$NHBoc** (black)

All amino terminal dendrimers were purified by size exclusion chromatography, and their structures confirmed by NMR (Figures S36-S38, S42-S44, S48-S50, S55-57 and S65-S67, ESI). As previously reported, characterization of dendrimers with high molecular weights and charges by MALDI-TOF is extremely difficult.[31,32] No mass spectrum could be obtained for described dendrimers, probably as a result of the lability of the *tert*-butyloxycarbonyl (BOC) protecting groups (in **Gn$_X$NHBoc** derivatives) and the high degree of positive charges (in **Gn$_X$NH$_2$** derivatives) during measurements.

Scheme 3. Synthesis of **G3$_{3AB}$NH$_2$** and **G3$_{Naph}$NH$_2$** dendrimers

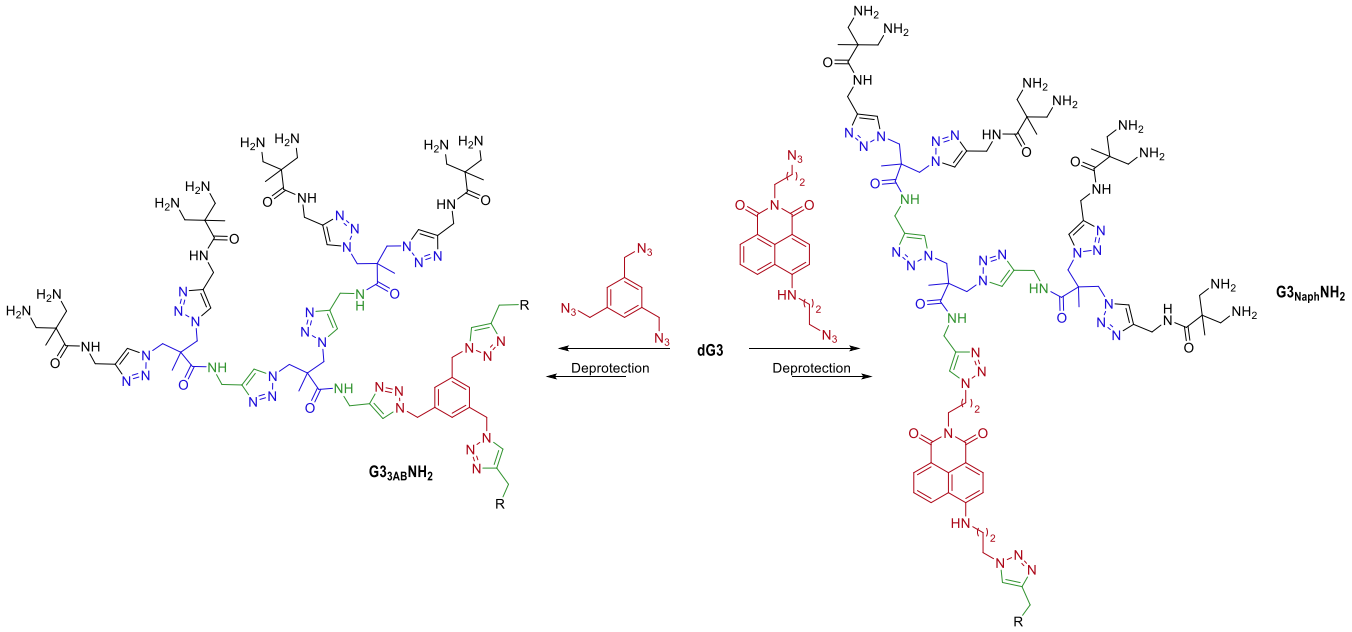

Reagents and conditions: $CuSO_4$, sodium ascorbate, water/*tert*-butyl alcohol (2:1) for click coupling; HCl 4M in dioxane, THF for amino deprotection.

As an alternative, in order to characterize the molecular weight and ensure the homogeneity of each generation of dendrimers, we used polyacrylamide gel electrophoresis (PAGE). Due to the structural similarity between dendrimers and basic proteins, the former can migrate on electrophoresis gels and be stained by reagents commonly used in PAGE.[33,34]

Figure 3 shows the electropherogram of the amino terminal dendrimers **G2$_{EDA}$NH$_2$**, **G3$_{EDA}$NH$_2$**, **G3$_{3AB}$NH$_2$** and **G3$_{Naph}$NH$_2$**, obtained on a 20% polyacrylamide gel. **G1$_{EDA}$NH$_2$** has not been included in the analysis since its molecular weight is relatively small for the standards used. It can be clearly seen in Figure 3 that the bands of all dendrimers (lanes 1, 2, 3 and 4) appear in the gel according to their molecular weight (Table 1) and in all cases resembles the homogeneity of the sample.

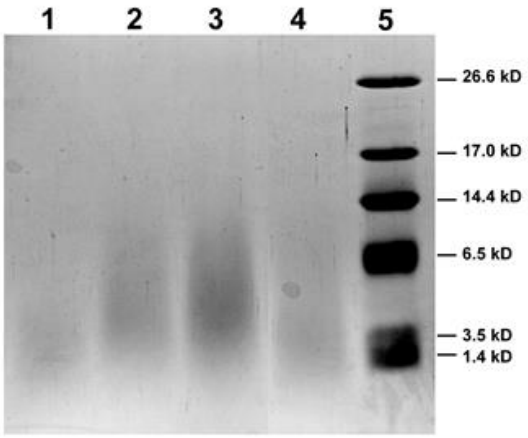

Figure 3. Electrophoresis of amine-terminated NH_2 dendrimers. Electrophoresis was performed on 20% polyacrylamide gel for 160 min at 125 V. Lane 1: **G2$_{EDA}$NH$_2$**; Lane 2: **G3$_{EDA}$NH$_2$**; Lane 3: **G3$_{3AB}$NH$_2$**; Lane 4: **G3$_{Naph}$NH$_2$**; Lane 5: Polypeptide SDS-PAGE Standards (BIO-RAD). The injected sample solution was 20 µg for each dendrimer. All dendrimers and Polypeptide SDS-PAGE Standards were stained uniformly with Coomassie Blue G-250 stain

Amino terminal dendrimers were examined by diffusion NMR techniques. DOSY (diffusion-ordered spectroscopy) experiments were carried out observing that the decays of all signals are monoexponential, resulting in a linear Stejskal-Tanner plot, which proves that the dendrimers were monodisperse (Figures S68-S72, ESI).[35] Diffusion coefficients (D) were also determined and used to estimate the size of all dendrimers in solution, by calculating the hydrodynamic radius (R_h) using the Stokes-Einstein equation (Table 1).[36,37]

Larger structures diffuse more slowly, showing smaller diffusion constants. As expected, the dendrimer radius increases with generation in dendrimers with the same core (**Gn$_{EDA}$NH$_2$**). This correlation is not so clear when comparing generation 3 dendrimers, probably due to a folding of the structure. **G3$_{Naph}$NH$_2$** shows a slightly higher diffusion constant than **G3$_{EDA}$NH$_2$**, which can be translated into a smaller size of the dendrimer. However, the inclusion in the structure of a third dendron, which implies a considerable increase in molecular weight, does not translate into a significant increase in the size of the dendrimer (Table 1). It is important to note that **G3-NH$_2$** dendrimers are built from different cores, whose structures and multiplicities influence not only the number of amino terminal groups but also the shape, morphology and size of the final dendrimers.

Molecular Dynamic Simulations

To obtain some information about the structure of these dendrimers, molecular models were created and simulated in water as explicit solvent using molecular dynamics (Figure 4). These compounds were built with three different residues: the respective core for each dendrimer (COR), the branched repeating fragment (REP), and the terminal ends (TAM), respectively (Figure S82, ESI). The equilibrated structures of these molecules have also been analyzed and several properties calculated (Table 1), such as the Radius of gyration (R_g), the aspect ratio and their asphericities.

Table 1. Data of prepared dendrimers. Diffusion coefficients (D) and hydrodynamic radius (R_h) determined by NMR experiments. Radius of gyration (R_g), aspect ratios (I_z/I_x and I_z/I_y) and asphericities (δ) calculated by MDS

Dendrimer	G1$_{EDA}$NH$_2$	G2$_{EDA}$NH$_2$	G3$_{EDA}$NH$_2$	G3$_{3AB}$NH$_2$	G3$_{Naph}$NH$_2$
Molecular Formula	$C_{18}H_{34}N_{12}O_2$	$C_{50}H_{86}N_{32}O_6$	$C_{114}H_{190}N_{72}O_{14}$	$C_{177}H_{288}N_{108}O_{21}$	$C_{128}H_{200}N_{74}O_{16}$
Terminal -NH$_2$ groups	4	8	16	24	16
M. W. (gmol^{-1})	450.55	1231.46	2793.26	4264.99	3031.51
D (m^{2}s^{-1})	$3.80{\cdot}10^{-10}$	$3.01{\cdot}10^{-10}$	$1.93{\cdot}10^{-10}$	$1.72{\cdot}10^{-10}$	$2.19{\cdot}10^{-10}$
R_h (Å)	5.27	6.66	10.38	11.65	9.15
R_g (Å)	4.17 ± 0.06	6.79 ± 0.09	10.51 ± 0.15	11.37 ± 0.16	9.93 ± 0.14
I_x/I_y	1.22 ± 0.07	1.20 ± 0.03	1.08 ± 0.03	1.27 ± 0.02	1.08 ± 0.03
I_x/I_z	1.62 ± 0.10	2.71 ± 0.16	3.79 ± 0.23	2.35 ± 0.12	2.85 ± 0.19
δ	0.019 ± 0.004	0.066 ± 0.006	0.103 ± 0.006	0.052 ± 0.005	0.073 ± 0.007

We found that the size of these molecules for the **Gn$_{EDA}$NH$_2$** series increases with each generation, as quantified from the DOSY experiments, and their values are in good agreement with the calculated radius of gyration (R_g) (Table 1). The fractal dimensionality (d_f) value for these compounds can be inferred from the relation between R_g and the number of the dendrimer's atoms (N) and has a value of 1.74 (Figure S83, ESI). This indicates that these dendrimer generations do not form perfect spheres since the fractal dimension for a perfectly spherical smooth surface is 3.[5]

The values of the three principal moments of inertia (I_x, I_y, I_z in decreasing order) can give information about the structural characteristics of these dendrimers. The ratios (I_x/I_y) and (I_x/I_z) are measures of the dendrimer's ellipsoid shape eccentricity. **Gn$_{EDA}$NH$_2$** dendrimers showed I_x/I_y and I_x/I_z ratios between 1.22-1.08 and 1.62-3.79 respectively (Table 1). The increase in the gap between the I_x/I_y and I_x/I_z values implies that the ellipsoidal shape is favored when the generation increases. This is corroborated by their asphericity values (Figure S84, ESI).

The atoms distribution within the dendrimers can be described using radial density profiles. Those corresponding to **Gn$_{EDA}$NH$_2$** dendrimer generations are shown in Figure S85, ESI. The maximum density is found to be close to the core of the dendrimers, decaying toward the edge. Second and third generation **Gn$_{EDA}$NH$_2$** dendrimers have a plateau corresponding with the distribution of the repetitive unit (REP) and decaying slowly toward the end of the molecule. This shows a region with low atom mobility, high localization and therefore with a dense dendrimer shell pattern. The number of terminal monomers (TAM) doubles with each generation, so the terminal amine groups extend over the molecule, always with increasing density toward the outer region of the dendrimer, but with a higher degree of terminal monomer back-folding when the generation increases (Figure S85, ESI).

To get more insight into how different cores affect the properties of these dendrimers, we have analyzed the calculated parameters for the **G3-NH$_2$** generations. The R_g of these dendrimers are similar and their values are within 1 Å and reproduce the experimental values (Table 1). The ellipsoid shape eccentricity displays I_x/I_y and I_x/I_z ratios between 1.08, 1.08, 1.27 and 3.79, 2.85, 2.35 for the EDA, Napth and 3AB cores, respectively (Table 1).

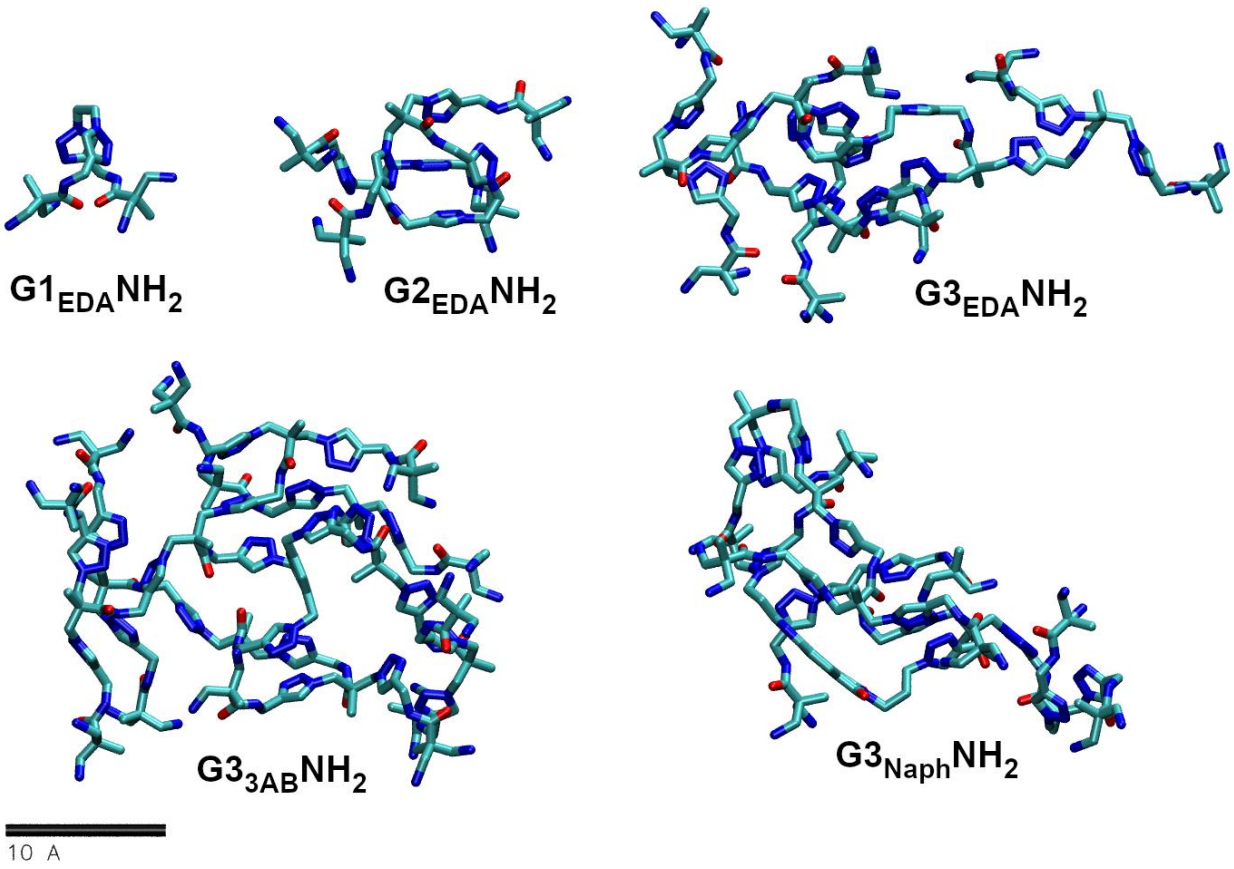

Figure 4. Snapshots from Molecular Dynamic Simulations of **G1$_{EDA}$NH$_2$, G2$_{EDA}$NH$_2$, G3$_{EDA}$NH$_2$, G3$_{3AB}$NH$_2$** and **G3$_{Naph}$NH$_2$**; (to simplify the picture, carbon atoms are depicted in cyan, oxygen atoms in red, nitrogen atoms in blue and hydrogens atoms are omitted)

The gap decrease between the I_x/I_y and I_x/I_z values implies that a more globular structure is favored when the number of atoms in the dendrimers increases, this is validated by the asphericity values (Table 1, TableS1 and Figure S86, ESI).

The radial density profiles for the **G3-NH₂** dendrimers are shown in Figure S87 (ESI). In these profiles, density is maxima around the core of the dendrimers. For EDA core-dendrimers, the density shows a plateau with a good correlation with the distribution of the repetitive unit REP and implies a dense dendrimer pattern. For 3AB and Napth core-dendrimers this plateau is smaller. The terminal amine groups are extended from the middle of the molecules toward the outside region of the dendrimer, except for the molecule with the 3AB core, which presents a high degree of back-folding and the TAM residue can be found along all the molecule (Figure S87, ESI). From all these dendrimers, the molecule with the Napth core has the least back-folding (Figure 4).

Comparing the family **$Gn_{EDA}NH2$** with others amino-terminal dendrimers (PAMAM,[5] PPI[38] and BAPAD[16]), the dendrimers of equivalent generation are similar in size, but differs in shape. While for PAMAM, PPI and BAPAD dendrimers are spheroids in shape when the generation growths, an ellipsoidal shape is favored when the generation of **$Gn_{EDA}NH2$** increases.

Luminescent properties of **$G3_{Naph}NH_2$**

$G3_{Naph}NH_2$ exhibits an intense fluorescence emission centered at 550 nm in aqueous solution (10^{-5} M, Figure 5a) with an excited state lifetime of 7.5 ns (λ_{em} = 550 nm). Although it has a quantum yield of 26 %, this value is unexpectedly considering an aqueous solution. Excitation and emission spectra acquired under two-photon excitation (TPE) conditions were also recorded (Figure 5a). The emission observed using an excitation wavelength of 880 nm coincides with the one obtained in the one-photon excitation (OPE) regime. When comparing these results with a model chromophore, similar results are observed. Emission and excitation spectra of *N*-(2-aminoethyl)-4-((2-aminoethyl)amino)-1,8-naphthalimide resembles the ones of the dendrimer Figure S80 (ESI), but possess a lower quantum yield (15%). **$G3_{Naph}NH_2$** becomes therefore an excellent tool for bioapplications where luminescence is required. The molecule combines the excellent properties of amino terminal dendrimers with a chromophore widely supported by its excellent photophysical properties.[39]

To evaluate the use of **$G3_{Naph}NH_2$** as a multichannel fluorescent marker for biological samples, a strain of *E. coli* bacteria was employed as a model target. The amino terminal groups of **$G3_{Naph}NH_2$** provide an effective binder to bacterial surface, owing to their capacity for hydrogen bonds and electrostatic interaction.[40] After incubation with a solution of the dendrimer, **$G3_{Naph}NH_2$** effectively labeled the *E. coli* cells as can be seen in Figure 5 (10^{-4} M) and Figure S81 (ESI) [$5{\cdot}10^{-4}$ M (500 µM)]. The outer surface of some bacteria shows an intense fluorescence under both OPE or TPE conditions, thus confirming the adhesion of the dendrimer to the bacterial wall. To further confirm that the origin of this fluorescence derives from the intrinsic emission of the naphthalimide core of the dendrimer, and to rule out biological sample autofluorescence and background noise,[41] specific controls were set up. In untreated bacteria no autofluorescence is observed under OPE or TPE conditions (the capture settings and image processing are identical).

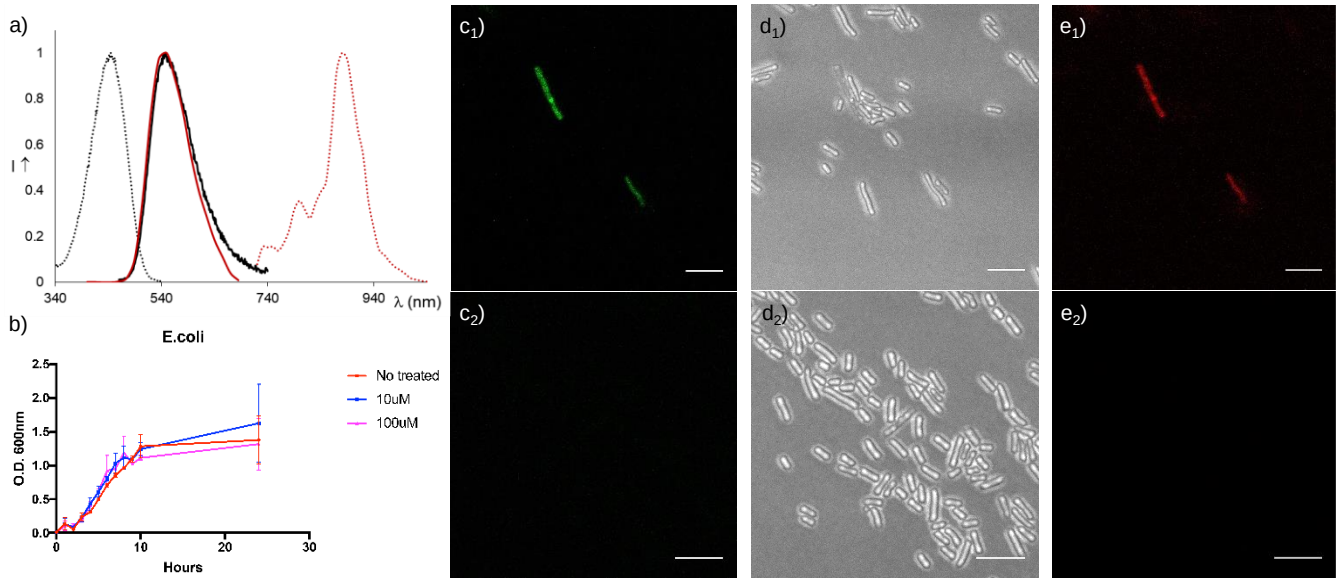

Figure 5. a) Excitation (dotted line) and emission (solid line) spectra of **$G3_{Naph}NH_2$** upon one-photon (black) or two-photon (red) excitation (450 nm and 880 nm respectively), in aqueous solutions. b) Growth curves for *E. coli* (bacteria were cultured in LB medium in the presence of different concentrations of **$G3_{Naph}NH_2$** (10 µM, blue; 100 µM, pink) or without **$G3_{Naph}NH_2$** (red). Confocal micrographs of *E. coli* incubated for 8 h with (upper row; c_1, d_1 and e_2) or without (bottom row; c_2, d_2 and e_2) **$G3_{Naph}NH_2$**: c_1, c_2) recorded emission with one photon excitation (λ_{exc} = 450 nm; collected through 500-600 nm); d_1, d_2) bright field images; e_1, e_2) recorded emission with two photon excitation (λ_{exc} = 880 nm; collected through 500-550 nm). Scale Bars: 5 µm

The dynamics of bacterial growth was monitored in liquid LB medium originally inoculated with 4_x10^6 *E. coli* and incubated in the presence (10 or 100 μM) or absence of $\mathbf{G3_{Naph}NH_2}$. No significant *E. coli* growth delay was recorded with increasing $\mathbf{G3_{Naph}NH_2}$ concentration from 10 to 100 μM (Figure 5b).

CONCLUSIONS

A new family of stable amino terminal dendrimers has been obtained combining protection/deprotection reactions and efficient CuAAC. In our convergent design, **dG3** dendron was prepared alternating click reactions, deprotections reactions, and amide formation, resulting in an effective synthesis where **dG3** can be obtained in large quantities with yields higher than 85% in all steps and with easy purification procedures. Different dendrimers have been obtained in one step from our highly versatile dendron. With this new methodology, it is possible to increase the number of amino terminal groups by choosing the appropriate multiplicity of the core. The size and shape of obtained dendrimers have been evaluated by NMR techniques. The data observed by DOSY experiments is well supported by fully atomistic Molecular Dynamic Simulations. The chemical structure of the core influences the shape and morphology of the final dendrimers, obtaining ellipsoidal shape from dendrimers with an alkyl core and a more globular shape in dendrimers with aromatic cores. We demonstrate that our effective dendron can be combined with suitable cores of different multiplicity, thus providing a powerful tool for the easy assembly of amino terminal dendrimers, with the desired molecular weight, shape and number of amino terminal groups. The chemical stability of these aliphatic-imidazole-amide dendrimers make them excellent candidates for biomedical applications. Moreover, inherent fluorescent dendrimer can be obtained in good yields, completely aqueous soluble and with the amino terminal groups intact. We also demonstrate the application in bioimaging of such dendrimers using both OPE and TPE conditions.

EXPERIMENTAL SECTION

All reactions were performed using commercially available reagents and solvents from the manufacturer without further purification. Chemicals were purchased from Sigma-Aldrich (L (+)-Ascorbic acid sodium salt, 3,3'-dichloropivalic acid, benzyl bromide, Pearlman's catalyst, 1,1′-carbonyldiimidazole, propargylamine, tris(bromomethyl)benzene, 4-bromo-1,8-naphthalic anhydride, 1,2-dibromoethane, 3-bromopropylamine hydrobromide), VWR Chemicals (sodium azide) or Alfa Aesar (HCl 4M in dioxane, triphenylphosphine, di-*tert*-butyl decarbonate) and used without further purification, unless otherwise indicated. Solvents were purchased from VWR Chemicals and Panreac. H2O was purified with a Mili-Q purification system from Millipore. Unless otherwise stated, all reactions were performed in air. Column chromatography and TLC were performed on silica gel 60 (0.040-0.063 mm) using UV light and/or stains to visualize the products. Sephadex™ G-10 pre-packed columns were used to purify the final dendrimers. ^{1}H and ^{13}C NMR spectra were measured in the indicated deuterated solvent at 25 °C on a Bruker Ascend 400 MHz spectrometer. Proton chemical shifts (δ) are reported with the solvent resonance employed as the internal standard ($CDCl_3$ δ 7.26, DMSO-d_6 δ 2.50, D_2O δ 4.79, MeOD-d_4 δ 3.31). Data are reported as follows: chemical shift, multiplicity, coupling constants (Hz) and integration. Carbon chemical shifts are reported in ppm with the solvent resonance as the internal standard ($CDCl_3$ δ 77.16, DMSO-d_6 δ 39.52, MeOD-d_4 δ 49.00). The HRMS (Electrospray Ionization Time of Flight, ESI-TOF) mass spectra (MS) were performed on a High Resolution Mass Spectrometer Orbitrap, Q-Exactive (Thermo Fisher Scientific, Waltham, MA, USA), in either positive or negative ion mode. Infrared (IR) spectra were recorded using a Jasco FT/IR-4100 spectrophotometer at ambient temperature. Hydrogenation reactions were carried out under hydrogen atmosphere (50 bar) using a Mini-Reactor from Erie-Autoclave Engineers. Luminescence measurements were performed using an Edinburgh Instruments FLS920 spectrometer equipped with a 450W Xenon lamp (Xe900) as continuous excitation source for stationary state measurements and Picoquant PLS-450 and PLS-500 pulsed LED diodes as pulsed excitation source for time-resolved measurements.

General procedure for *click* reactions. Azido-compound (1 eq), alkyne (1.1 eq per azido group), Copper (II) Sulphate 5-hydrate (0.01 eq per azido group) and L (+)-Ascorbic acid Sodium salt (0.1 eq per azido group) were dissolved in a *tert*-butanol/water 1:2 mixture. The mixture was stirred at room temperature for one week. Afterwards, the solvent was removed using rotatory evaporation. NH_3 aq. (50 mL) and dichloromethane (50 mL) were added and the phases were separated. The aqueous phase was extracted with CH_2Cl_2 (3 × 30 mL). The combined organic layers were washed with NH_3 aq./Brine 1:1 (3 × 80 mL). The organic layer was dried over $MgSO_4$ anh. and the solvent was removed by rotary evaporation. The product was purified by precipitation in n-hexane.

General procedure for deprotection of amines. The compounds were dissolved in THF (10 mL) and the solution was cooled in an ice-water bath. HCl 4M in dioxane (10 mL) was added dropwise and the mixture was stirred overnight. Afterwards, the solvent was evaporated under vacuum. The compounds were purified by sephadex column.

Synthesis of 3,3′-diazidopivalic acid. Sodium azide (7.50 g, 115 mmol, 4 eq) was added to a solution of 3,3'-dichloropivalic acid(5.00 g, 29 mmol, 1 eq) in DMF/H_2O 9:1 (20 mL). The resulting solution was heated in a heat block at 80°C overnight. The solvent was removed under vacuum and ethyl acetate (50 mL) was added to promote the precipitation of the remaining sodium azide. The solution was left in the refrigerator overnight. Then the mixture was filtered and the solvent was removed under vacuum to obtain the product (4.80 g, 26.1 mmol, 90%) as a colorless oil. ^{1}H-NMR (400 MHz, $CDCl_3$) δ ppm: 3.63 (d, J = 12.3 Hz, 2 H), 3.52 (d, J = 12.3 Hz, 2 H), 1.27 (s, 3 H). ^{13}C{^{1}H} NMR (100 MHz,

$CDCl_3$) δ: 179.8, 54.6, 47.6, 19.4. HRMS calcd. for $C_5H_7N_6O_2^-$ 183.0625 $[M - H]^-$, found 183.0626.

Synthesis of benzyl-3,3′-diazidopivaloate. To a solution of 3,3′-diazidopivalic acid (5.00 g, 27 mmol, 1 eq) in DMF (20 mL) was added sodium carbonate (4.29 g, 40.5 mmol, 1.5 eq) and benzyl bromide (4.8 mL, 40.5 mmol, 1.5 eq). The mixture was stirred for overnight at room temperature. Then, n-hexane (100 mL) and water (50 mL) were added and the phases were separated. The organic layer was washed with water (3 × 50mL), dried over $MgSO_4$ anh. and the solvent was removed under vacuum. Purification was performed by silica gel column chromatography (n-hexane/ethyl acetate, 9:1 v/v) to obtain the product (6.67 g, 24.3 mmol, 90%) as a colorless oil. ^{1}H NMR (400 MHz, $CDCl_3$) δ: 7.42 – 7.32 (m, 5 H), 5.19 (s, 2 H), 3.63 (d, J = 12.2 Hz, 2 H), 3.52 (d, J = 12.2 Hz, 2 H) 1.24 (s, 3 H). ^{13}C{^{1}H} NMR (100 MHz, $CDCl_3$) δ: 173.1, 135.4, 128.8, 128.6, 128.3, 67.3, 54.9, 47.8, 19.4. HRMS calcd. for $C_{12}H_{14}N_6O_2Na^+$ 297.1070 $[M + Na]^+$, found 297.1072.

Synthesis of benzyl-3,3′-diaminopivaloate. Benzyl-3,3′-diazidopivaloate (2.00 g, 7.30 mmol, 1 eq) was dissolved in THF (20 mL) and placed in an ice bath. Triphenylphosphine (10.2 g, 38.6 mmol, 5.3 eq) was dissolved in THF (10 mL) and added dropwise to the previous solution. The mixture was left under reflux in a heat block overnight. Afterwards, 1.5 mL of water were added and the reaction was left under reflux for another day. Then, THF was removed under vacuum and the product was dissolved in HCl 1M (10 mL). The aqueous phase was washed with dichloromethane (5 × 30 mL). The water was later removed under vacuum to obtain the desired compound (2.11 g, 7.15 mmol, 98%) as a colorless solid; mp 160–162 °C. ^{1}H NMR (400 MHz, D_2O) δ: 7.56 - 7.43 (m, 5 H), 5.35 (s, 2 H), 3.45 (d, J = 13.7 Hz, 2 H), 3.29 (d, J = 13.7 Hz, 2 H), 1.49 (s, 3 H). ^{13}C{^{1}H} NMR (100 MHz, MeOD-d_4) δ: 173.2, 136.3, 129.63, 129.61, 129.59, 69.4, 45.0, 44.34, 19.4. HRMS calcd. for $C_{12}H_{19}N_2O_2^+$ 223.1441 $[M + H]^+$, found 223.1441.

Synthesis of benzyl-3,3′-bis(*tert*-butoxycarbonyl)aminopivaloate. To an ice-cooled solution of benzyl-3,3′-diaminopivaloate (2.07 g, 7.00 mmol, 1 eq) in H_2O/acetone 1:1 (20 mL), NaOH 1M was added dropwise until pH>10 was achieved. Di-*tert*-butyl dicarbonate (3.05 mg, 15.40 mmol, 2 eq) was then added and the reaction was stirred overnight at room temperature. The product was extracted using dichloromethane (5 × 30mL). The organic phase was dried with $MgSO_4$ anh. and the solvent was removed under vacuum to obtain the product (2.84 mg, 6.72 mmol, 96%) as a colorless oil. ^{1}H NMR (400 MHz, $CDCl_3$) δ: 7.39-7.30 (m, 5 H), 5.14 (s, 2 H), 3.48 (dd, J = 14.4, 8.6 Hz, 2 H), 3.12 (dd, J = 14.4, 5.2 Hz, 2 H), 1.43 (s, 18 H), 1.14 (s, 3 H). ^{13}C{^{1}H} NMR (100 MHz, $CDCl_3$) δ: 175.2, 156.7, 135.8, 128.7, 128.4, 128.0, 79.4, 66.7, 48.9, 43.5, 28.4, 19.0. HRMS calcd. for $C_{22}H_{34}N_2O_6Na^+$ 445.2309 $[M + Na]^+$, found 445.2309.

Synthesis of 3,3′-bis(*tert*-butoxycarbonyl)aminopivalic acid. To a solution of benzyl-3,3′-(*tert*-butoxycarbonyl)aminopivaloate (400 mg, 0.95 mmol, 1 eq) in methanol (10 mL), Pearlman's catalyst (100 mg, 0.71 mmol, 0.7 eq) is added. After hydrogenation for two hours, the catalyst was removed by filtration through MeOH-pre-wetted Celite. The solvent was removed under vacuum to obtain the desired compound (309 mg, 0.93 mmol, 98%) as a colorless oil. ^{1}H NMR (400 MHz, MeOD-d_4) δ: 3.25 (d, J = 14.2 Hz, 2 H), 3.17 (d, J = 14.2 Hz, 2 H), 1.43 (s, 18 H) 1.07 (s, 3 H). ^{13}C{^{1}H} NMR (100 MHz, DMSO-d_6) δ: 180.0, 158.7, 80.2, 46.7, 45.5, 28.7, 19.6. HRMS calcd. for $C_{15}H_{28}N_2O_6Na^+$ 355.1840 $[M + Na]^+$, found 355.1838.

Synthesis of dG1. A solution of 3,3′-(*tert*-butoxycarbonyl)aminopivalic acid (1.70 g, 5.11 mmol, 1eq) in anhydrous acetonitrile (5 mL) was added to a solution of 1,1′-carbonyldiimidazole (CDI) (1.3 g, 7.66 mmol, 1.5 eq) in anhydrous acetonitrile (15 mL) and the mixture was stirred at room temperature for one hour. Afterwards, propargylamine (0.7 mL, 10.22 mmol, 2 eq) was added and the stirring mixture was left overnight at room temperature. The solvent was removed under vacuum. The residue was dissolved in dichloromethane (50 mL) and washed with HCl 0.05M (3 × 50 mL). The combined organic phase was dried with $MgSO_4$ anh., filtered and concentrated under reduced pressure to obtain the product (1.57 g, 4.24 mmol, 83 %) as a colorless solid; mp 70–71 °C. ^{1}H-NMR (400 MHz, DMSO-d_6) δ ppm: 3.80 (dd, J = 4.8, 2.1 Hz, 2 H), 3.14-3.01 (m, 5 H), 1.37 (s, 18 H), 0.95 (s, 3 H). ^{13}C{^{1}H} NMR (100 MHz, DMSO-d_6) δ ppm: 173.9, 156.1, 81.3, 78.0, 72.7, 47.6, 44.3, 28.4, 28.2, 18.5. HRMS calcd. for $C_{18}H_{31}N_3O_5Na^+$ 392.2161 $[M + Na]^+$, found 392.2164.

Synthesis of dG2-CO_2Bn. This compound was obtained from benzyl-3,3′-diazidopivaloate (418 mg, 1.53 mmol, 1 eq), **dG1** (1.23 g, 3.37 mmol, 2.2 eq), Copper (II) Sulphate 5-hydrate (10 mg, 0.04 mmol, 0.02 eq) and L(+)-ascorbic acid sodium salt (32 mg, 0.16 mmol, 0.1 eq) in *tert*-butanol/water 1:2 (10 mL) to obtain the product (1.34 g, 1.32 mmol, 87%) as a colorless powder; mp 111–113 °C. ^{1}H-NMR (400 MHz, DMSO-d_6) δ ppm: 7.79 (s, 2 H), 7.40-7.32 (m, 5 H), 5.09 (s, 2 H),), 4.72 (d, J = 14.2 Hz, 2 H),), 4.59 (d, J = 14.1 Hz, 2 H), 4.27 (d, J = 4.8 Hz, 4 H), 3.16-3.04 (m, 8 H), 1.35 (s, 36 H), 1.00 (s, 3 H), 0.96 (s, 6 H). ^{13}C{^{1}H} NMR (100 MHz, DMSO-d_6) δ ppm: 174.1, 171.8, 156.1, 145.0, 135.3, 128.4, 128.1, 128.0, 124.2, 77.9, 66.8, 53.4, 48.3, 47.6, 44.4, 34.6, 28.1, 18.4, 17.7. HRMS calcd. for $C_{48}H_{77}N_{12}O_{12}^+$ 1013.5784 $[M + H]^+$, found 1013.5781.

Synthesis of dG2-CO_2H. A solution of **dG2-CO_2Bn** (1.76 g, 1.74 mmol, 1 eq) in MeOH (10 mL) was added to $Pd(OH)_2$ (100 mg, 0.71 mmol, 0.3 eq). Hydrogenation took place in a hydrogenation reactor at room temperature and 50 bar hydrogen pressure. After five hours, the catalyst was removed by filtration through MeOH-pre-wetted Celite. The solvent was removed under vacuum to obtain the product (1.61 mg, 1.71 mmol, 98%) as a solid (compound decomposes above 210 °C). ^{1}H-NMR (400 MHz, DMSO-d_6) δ ppm: 7.92 (s, 2 H), 4.51 (d, J = 13.7 Hz, 2 H), 4.35 (d, J = 13.7 Hz, 2 H), 4.27 (s, 4 H), 3.16-3.04 (m, 8 H), 1.35 (s, 36 H), 0.96 (s, 6 H), 0.81 (s, 3 H). ^{13}C{^{1}H} NMR (100 MHz, DMSO-d_6) δ ppm: 174.2, 174.1, 156.2, 144.6, 124.0, 77.9, 54.3, 48.5, 47.7, 44.4, 34.6, 28.1, 19.1, 18.5. HRMS calcd. for $C_{41}H_{70}N_{12}O_{12}Na^+$ 945.5134 $[M + Na]^+$, found: 945.5124.

Synthesis of compound dG2. A solution of **dG2-CO_2H** (2.78 g, 3.02 mmol, 1 eq) in anhydrous acetonitrile (15 mL) was added to a solution of CDI (734 mg, 4.53 mmol, 1.5 eq) in anhydrous acetonitrile (45 mL) and the mixture was stirred at room temperature for one hour. Afterwards, propargylamine (0.3 mL, 4.53 mmol, 1.5 eq) was added and the stirring mixture was left overnight at room temperature. The solvent was removed under vacuum. The residue was dissolved in dichloromethane (50 mL) and washed with HCl 0.05M (5 × 50 mL). The combined organic phase was dried with $MgSO_4$ anh., filtered and concentrated under reduced pressure to obtain the product (2.46 g, 2.57 mmol, 85 %) as a colorless solid (compound decomposes above 105 °C). ^{1}H-NMR (400 MHz, DMSO-d_6) δ ppm: 7.22 (s, 2 H), 4.66 (d, J = 14.1 Hz, 2 H), 4.52 (d, J = 14.1 Hz, 2 H), 4.27 (d, J = 5.1 Hz, 4 H), 3.83 (d, J = 2.7 Hz, 2 H), 3.12-3.07 (m, 8 H), 1.76 (s, 1 H), 1.36 (s, 36 H), 0.96 (s, 6 H), 0.93 (s, 3 H). ^{13}C{^{1}H} NMR (100 MHz, DMSO-d_6) δ ppm: 174.1, 171.3, 156.1, 144.9, 123.9, 78.0, 73.1, 67.0, 53.9, 48.0, 47.6, 44.4, 34.6, 28.1, 18.4, 17.4. HRMS calcd. for $C_{44}H_{73}N_{13}O_{11}Na^+$ 982.5450 [M + Na]$^+$, found: 982.5447.

Synthesis of dG3-CO_2Bn. This compound was obtained from benzyl-3,3′-diazidopivaloate (320 mg, 1.17 mmol, 1 eq), **dG2** (2.47 g, 2.58 mmol, 2.2 eq), copper (II) sulphate 5-hydrate (6 mg, 0.02 mmol, 0.02 eq) and L(+)-ascorbic acid sodium salt (24 mg, 0.12 mmol, 0.1 eq) in *tert*-butanol/water 1:2 (27 mL) to obtain the desired product (2.31 g, 1.05 mmol, 90%) as a colorless solid (compound decomposes above 149 °C). ^{1}H-NMR (400 MHz, DMSO-d_6) δ ppm: 7.94-7.75 (m, 6 H), 7.36-7.32 (m, 5 H), 5.10 (s, 2 H), 4.80 (d, J = 14.2 Hz, 2 H), 4.65 (d, J = 14.2 Hz, 4 H), 4.51 (d, J = 14.0 Hz, 4 H), 4.44 (d, J = 13.7 Hz, 2 H), 4.31-4.18 (m, 12 H), 3.18-3.04 (m, 16 H), 1.35 (s, 72 H), 0.96-0.93 (m, 21 H). ^{13}C{^{1}H} NMR (100 MHz, DMSO-d_6) δ ppm: 174.2, 171.8, 171.4, 156.1, 144.9, 144.2, 135.3, 128.4, 128.1, 128.0, 126.4, 124.0, 78.0, 66.8, 53.8, 53.5, 48.4, 47.9, 47.6, 44.4, 34.8, 34.6, 28.1, 18.4, 17.8, 17.6. HRMS calcd. for $C_{100}H_{160}N_{32}O_{24}Na^+$ 2216.2181 [M + Na]$^+$, found: 2216.2263.

Synthesis of dG3-CO_2H. A solution of **dG3-CO_2Bn** (1.18 g, 0.54 mmol, 1 eq) in MeOH (10 mL) is added to $Pd(OH)_2$ (23 mg, 0.16 mmol, 0.3 eq). After hydrogenating for 6 days, the catalyst was removed by filtration through MeOH-prewetted Celite. The solvent was removed under vacuum to obtain the product (966 mg, 0.46 mmol, 85%) as a solid (compound decomposes above 230 °C). ^{1}H-NMR (400 MHz, DMSO-d_6) δ ppm: 8.18-7.54 (m, 6 H), 4.72-4.44 (m, 12 H), 4.37-4.22 (m, 12 H), 3.16-2.96 (m, 16 H), 1.36 (s, 72 H), 0.96 (s, 12 H), 0.95 (s, 6 H), 0.81 (s, 3 H). ^{13}C{^{1}H} NMR (100 MHz, DMSO-d_6) δ ppm: 174.3, 174.2, 171.1, 156.2, 145.0, 144.5, 123.9, 123.9, 77.9, 54.7, 53.9, 48.7, 47.6, 47.5, 44.4, 34.6, 34.5, 28.1, 19.0, 18.5, 17.6. HRMS calcd. for $C_{93}H_{153}N_{32}O_{24}^-$ 2102.1735 [M – H]$^-$, found: 2102.1636.

Synthesis of dG3. A solution of **dG3-CO_2H** (1.10 g, 0.52 mmol, 1 eq) in anhydrous acetonitrile (10 mL) was added to a solution of CDI (126 mg, 0.78 mmol, 1.5 eq) in anhydrous acetonitrile (10 mL) and the mixture was stirred at room temperature for one hour. Afterwards, propargylamine (52 µL, 0.78 mmol, 1.5 eq) was added and the stirring mixture was left overnight at room temperature. The solvent was removed under vacuum and the residue was dissolved in dichloromethane (30 mL) and washed with HCl 0.05M (5 × 30mL). The combined organic phase were dried with $MgSO_4$ anh., filtered and concentrated under reduced pressure to obtain the product (723 mg, 0.34 mmol, 65 %) as a colorless solid (compound decomposes above 146 °C). ^{1}H-NMR (400 MHz, DMSO-d_6) δ ppm: 7.93-7.54 (m, 6 H), 4.71-4.53 (m, 12 H), 4.39-4.15 (m, 12 H), 3.83 (s, 2 H), 3.20-2.95 (m, 16 H), 1,74 (s, 1 H), 1.35 (s, 72 H), 0.96-0.93 (m, 21 H). ^{13}C{^{1}H} NMR (100 MHz, DMSO-d_6) δ ppm: 174.2, 171.5, 171.4, 156.2, 144.9, 144.2, 124.2, 124.0, 78.0, 73.1, 53.88, 53.92, 53.8, 51.4, 48.0, 47.9, 47.6, 44.4, 34.6, 28.6, 28.2, 18.5, 17.6, 17.4. HRMS calcd. for $C_{96}H_{159}N_{33}O_{23}^{2+}$ 2142.2287 [M + 2 H]$^{2+}$, found: 1071.1137.

Synthesis of 1,2-diazidoethane. 1,2-diazidoethane was synthesized as described in literature.[28] ^{1}H-NMR (400 MHz, $CDCl_3$) δ ppm: 3.46 (s, 4 H). ^{13}C{^{1}H} NMR (100 MHz, $CDCl_3$) δ ppm: 50.7.

Synthesis of $G1_{EDA}$NHBoc. dG1 (500 mg, 1.36 mmol, 2.2 eq), 1,2-diazidoethane (69 mg, 0.62 mmol, 1 eq), copper (II) sulphate 5-hydrate (3 mg, 0.01 mmol, 0.02 eq) and L(+)-ascorbic acid sodium salt (12 mg, 0.06 mmol, 0.1 eq) in *tert*-butanol/water 1:2 (18 mL) to obtain the product (485 mg, 0.57 mmol, 92 %) as a colorless oil. ^{1}H-NMR (400 MHz, DMSO-d_6) δ ppm: 7.76 (s, 2 H), 4.82 (s, 4 H), 4.24 (d, J = 5.2 Hz, 4 H), 3.18-2.98 (m, 8 H), 1.36 (s, 36 H), 0.96 (s, 6 H). ^{13}C{^{1}H} NMR (100 MHz, DMSO-d_6) δ ppm: 174.1, 156.1, 145.3, 122.9, 78.0, 48.9, 47.6, 44.4, 34.6, 28.1, 18.4. HRMS calcd. for $C_{38}H_{66}N_{12}O_{10}Na^+$ 873.4923 [M + Na]$^+$, found: 873.4921.

Synthesis of $G1_{EDA}NH_2$. This compound was obtained from **$G1_{EDA}$NHBoc** (450 mg, 0.53 mmol) to obtain the desired product (309 mg, 0.52 mmol, 98%) as a colorless solid. ^{1}H-NMR (400 MHz, D_2O) δ ppm: 7.85 (s, 2 H), 4.94 (s, 4 H), 4.49 (s, 4 H), 3.34 (d, J = 13.5 Hz, 4 H), 3.15 (d, J = 13.5 Hz, 4 H), 1.42 (s, 6 H). ^{13}C{^{1}H} NMR (100 MHz, D_2O) δ ppm: 173.1, 143.7, 123.2, 49.2, 44.2, 43.3, 33.8, 16.6.

Synthesis of $G2_{EDA}$NHBoc. dG2 (1.09 g, 1.14 mmol, 2.2 eq), 1,2-diazidoethane (58 mg, 0.52 mmol, 1 eq), copper (II) sulphate 5-hydrate (3 mg, 0.01 mmol, 0.02 eq) and L(+)-ascorbic acid sodium salt (10 mg, 0.06 mmol, 0.1 eq) in *tert*-butanol/water 1:2 (18 mL) to obtain the product (845 mg, 0.42 mmol, 80 %) as a colorless solid (compound decomposes above 140 °C). ^{1}H-NMR (400 MHz, DMSO-d_6) δ ppm: 8.55-7.72 (m, 6 H), 4.90 (d, J = 14.7 Hz, 4 H), 4.66 (d, J = 13.9 Hz, 4 H), 4.51 (d, J = 14.1 Hz, 4 H), 4.30-4.14 (m, 12 H), 3.24-3.00 (m, 16 H), 1.35 (s, 72 H), 0.96 (s, 12 H), 0.93 (s, 6 H). ^{13}C{^{1}H} NMR (100 MHz, DMSO-d_6) δ ppm: 174.1, 171.4, 156.1, 144.9, 144.6, 124.0, 123.4, 78.0, 53.8, 49.0, 47.9, 47.6, 44.4, 34.8, 34.6, 28.1, 18.4, 17.5.

Synthesis of $G2_{EDA}NH_2$. This compound was obtained from **$G2_{EDA}$NHBoc** (400 mg, 0.20 mmol) to obtain the product (299 mg, 0.20 mmol, 98 %) as a colorless solid. ^{1}H-NMR (400 MHz, D_2O) δ ppm: 7.78-7.66 (m, 6 H), 5.02 (s, 4 H), 4.58-4.43 (m, 12 H), 4.31 (s, 8 H), 3.33 (d, J = 13.2 Hz, 8 H), 3.15 (d, J = 13.5 Hz, 8 H), 1.41 (s, 12 H), 1.13 (s, 6 H). ^{13}C{^{1}H} NMR (100 MHz, D_2O) δ ppm: 173.2, 172.4, 143.6, 143.1, 124.2, 123.8, 54.1, 49.2, 47.9, 44.3, 43.4, 34.0, 33.8, 16.7, 15.8.

Synthesis of $G3_{EDA}NHBoc$. This compound was obtained from **dG3** (179 mg, 0.084 mmol, 2.2 eq), 1,2-diazidoethane (4 mg, 0.04 mmol, 1 eq), copper (II) sulphate 5-hydrate (0.2 mg, 0.001 mmol, 0.02 eq) and L(+)-ascorbic acid sodium salt (2 mg, 0.01 mmol, 0.1 eq) in *tert*-butanol/water 1:2 (6 mL) to obtain the desired product (163 mg, 0.04 mmol, 93 %) as a colorless solid (compound decomposes above 145 °C). ^{1}H-NMR (400 MHz, DMSO-d_6) δ ppm: 7.97-7.77 (m, 14 H), 4.90 (s, 4 H), 4.68-4.57 (m, 24 H), 4.43-4.16 (m, 28 H), 3.22-2.98 (m, 32 H), 1.34 (s, 144 H), 1.08-0.88 (m, 42 H). ^{13}C{^{1}H} NMR (100 MHz, DMSO-d_6) δ ppm: 174.2, 171.48, 171.49, 156.2, 145.1, 145.0, 144.9, 124.2, 124.1, 124.0,78.0, 53.8, 51.4, 48.4, 47.9, 47.7, 47.4, 44.4, 34.6, 34.59, 34.57,28.1, 18.5, 17.7, 17.6.

Synthesis of $G3_{EDA}NH_2$. This compound was obtained from **$G3_{EDA}$NHBoc** (109 mg, 0.025 mmol) to obtain the product (82 mg, 0.025, 98 %) as a colorless solid. ^{1}H-NMR (400 MHz, D_2O) δ ppm: 8.04-7.62 (m, 14 H), 5.01 (s, 4 H), 4.66-4.20 (m, 44 H), 3.85-3.56 (m, 8 H), 3.44-3.09 (m, 32 H), 1.45 (s, 24 H), 1.16 (s, 12 H), 1.00 (s, 6 H). ^{13}C{^{1}H} NMR (100 MHz, D_2O) δ ppm: 174.0, 173.0, 172.4, 143.2, 143.1, 143.0, 123.93, 123.90, 123.88, 54.7, 54.2, 49.2, 48.1, 44.2, 44.0, 43.2, 34.0, 33.83, 33.77, 16.5, 16.4, 15.9.

Synthesis of 1,3,5-tris(azidomethyl)benzene. 1,3,5-tris(azidomethyl)benzene was synthesized as described.[30] ^{1}H-NMR (400 MHz, $CDCl_3$) δ ppm: 7.25 (s, 3 H), 4.40 (s, 6H).

Synthesis of $G3_{3AB}NHBoc$. This compound was obtained from **dG3** (179 mg, 0.084 mmol, 3.3 eq), 1,3,5-tris(azidomethyl)benzene (6 mg, 0.025mmol, 1 eq), copper (II) sulphate 5-hydrate (0.2 mg, 0.001 mmol, 0.03 eq) and L(+)-ascorbic acid sodium salt (3 mg, 0.01 mmol, 0.3 eq) in *tert*-butanol/water 1:2 (6 mL) to obtain the product (98 mg, 0.015 mmol, 59 %) as a colorless solid (compound decomposes above 140 °C). ^{1}H-NMR (400 MHz, DMSO-d_6) δ ppm: 7.97-7.77 (m, 24 H), 5.63-5.56 (m, 6 H), 4.77-4.45 (m, 36 H), 4.39-4.14 (m, 42H), 3.22-2.93 (m, 48 H), 1.34 (s, 216 H), 1.06-0.88 (m, 54 H). ^{13}C{^{1}H} NMR (100 MHz, DMSO-d_6) δ ppm: 174.2, 172.4, 171.4, 156.2, 145.1, 144.9, 144.6, 137.1, 127.5, 124.04, 123.95, 123.4, 78.0, 53.8, 48.4, 47.9, 47.8, 47.7, 47.6, 47.4, 44.4, 35.9, 34.9, 34.6, 28.1, 18.5, 18.0, 17.7.

Synthesis of $G3_{3AB}NH_2$. This compound was obtained from **$G3_{3AB}$NHBoc** (50 mg, 0.008mmol) to obtain the product (40 mg, 0.008 mmol, 98%) as a colorless solid in a quantitative way. ^{1}H-NMR (400 MHz, D_2O) δ ppm: 8.10-7.62 (m, 21 H), 7.26 (s, 3 H), 5.65 (m, 6 H), 4.67-4.18 (m, 66 H), 3.71-3.52 (m, 6H), 3.47 (d, J = 13.6 Hz, 24 H), 3.23 (d, J = 13.5 Hz, 24 H), 3.14-2.93 (m, 6 H), 1.50 (s, 36 H), 1.16 (s, 18 H) 1.01 (s, 9 H). ^{13}C{^{1}H} NMR (100 MHz, D_2O) δ ppm: 172.3, 172.1, 170.3, 143.0, 142.9, 142.8, 124.3, 124.2, 124.1, 54.2, 49.0, 48.1, 48.0, 47.8, 43.6, 42.7, 34.0, 33.9, 33.8, 16.3, 15.9, 15.8.

Synthesis of 3-azidopropylamine. 3-Bromopropylamine hydrobromide (5.00 g, 22.84 mmol, 1 eq) was dissolved in water (10 mL) and sodium azide was added (4.45 g, 68.52 mmol, 3 eq). The reaction was stirred during three days at 80ºC in a heat block. The mixture was cooled in an ice-water bath and ether was added (20 mL). Potassium hydroxide pellets were added until basic pH was attained. The organic layer was separated and the aqueous phase was extracted with ether (3 × 20 mL). The combined organic layers were dried with $MgSO_4$ anh. and concentrated to obtain the product (1.14 g, 11.42 mmol, 50 %) as a colorless oil. ^{1}H-NMR (400 MHz, D_2O) δ ppm: 3.67 (t, J = 7.5 Hz, 2 H), 3.24 (t, J = 6.8 Hz, 2 H), 2.11 (Q, J= 6.8 Hz, 2 H).

Synthesis of N-(3-azidopropyl)-4-((3-azidopropyl)amino)-1,8-naphthalimide. A solution of 4-bromo-1,8-naphthalic anhydride (500 mg, 1.80 mmol, 1 eq) and 3-azidopropylamine (2.7 g, 27 mmol, 15 eq) in DMSO (2.5 mL) was heated in a heat block at 80ºC overnight. Then, dichloromethane was added (50 mL) and the mixture was washed with HCl (3 × 30 mL). The organic layer was dried using $MgSO_4$ anh. and was concentrated. Purification was performed by silica gel column chromatography (dichloromethane:methanol, 99:1 v/v) to obtain the product (4.23 g, 1.22 mmol, 68 %) as a yellow solid (compound decomposes above 171 °C). ^{1}H-NMR (400 MHz, $CDCl_3$) δ ppm: 8.57 (d, J = 7.3 Hz, 1 H), 8.45 (d, J = 8.4 Hz, 1 H), 8.09 (d, J = 8.1 Hz, 1 H), 7.62 (t, J = 8.1 Hz, 1 H), 6.71 (d, J = 8.5 Hz, 1 H), 4.25 (t, J = 7 Hz, 2 H), 3.69-3.49 (m, 4 H), 3.41 (t, J = 7 Hz, 2 H), 2.18-1.93 (m, 4 H). ^{13}C{^{1}H} NMR (100 MHz, $CDCl_3$) δ ppm: 164.8, 164.2, 149.4, 134.6, 131.4, 129.9, 126.1, 125.1, 123.1, 120.5, 110.6, 104.4, 49.9, 49.6, 41.8, 37.7, 28.0, 27.9. HRMS calcd. for $C_{18}H_{19}N_8O_2^-$ 379.1631 $[M + H]^+$, found: 379.1625.

Synthesis of $G3_{Naph}NHBoc$. This compound was obtained from **dG3** (179 mg, 0.084 mmol, 2.2 eq), N-(3-azidopropyl)-4-((3-azidopropyl)amino)-1,8-naphthalimide (14 mg, 0.04 mmol, 1 eq), copper (II) sulphate 5-hydrate (0.2 mg, 0.001 mmol, 0.02 eq) and L(+)-ascorbic acid sodium salt (2 mg, 0.01 mmol, 0.1 eq) in *tert*-butanol/water 1:2 (6 mL) to obtain the product (107 mg, 0.02 mmol, 58 %) as a yellow solid (compound decomposes above 126 °C). ^{1}H-NMR (400 MHz, DMSO-d_6) δ ppm: 8.14-7.59 (m, 19 H), 4.77-4.04 (m, 56 H), 3.52 (s, 2H), 3.21-2.94 (m, 34 H), 2.34-2.15 (m, 2 H), 2.01-1.83 (m, 2 H) 1.35 (s, 144 H), 1.08-0.88 (m, 42 H). ^{13}C{^{1}H} NMR (100 MHz, DMSO-d_6) δ ppm: 174.2, 172.4, 171.5, 163.9, 163.1, 156.2, 150.7, 145.1, 145.0, 144.9, 134.3, 130.8, 129.5, 129.0, 128.9, 128.3, 124.3, 124.0, 121.9, 120.3, 107.9, 103.8, 78.0, 53.9, 53.5, 48.9, 48.6, 48.4, 48.0, 47.7, 44.4, 37.0, 35.6, 34.9, 34.6, 34.6, 28.2, 27.2, 27.2, 18.5, 17.7, 17.6.

Synthesis of $G3_{Naph}NH_2$. This compound was obtained from **$G3_{Naph}$NHBoc** (67 mg, 0.014mmol) to obtain the product (50 mg, 0.014 mmol, 98 %) as a yellow solid. UV (H_2O): λ_{max} nm (ε): 259 (4709), 284 (4125), 447 (3209). ^{1}H-NMR (400 MHz, D_2O) δ ppm: 8.05-7.62 (m, 19 H), 4.65-4.23 (m, 44 H), 3.75 (d, J = 13.6 Hz, 4 H), 3.66 (d, J = 11.6 Hz, 4 H), 3.60-3.49 (m, 4 H), 3.41 (d, J = 13.2 Hz, 16 H), 3.20 (d, J = 10.1 Hz, 16 H), 3.11-2.89 (m, 4 H), 1.46 (s, 24 H), 1.16 (s, 12 H), 1.00 (s, 6H). ^{13}C{^{1}H} NMR (100 MHz, D_2O) δ ppm: 172.64, 172.57, 172.3, 143.02, 143.05, 143.11, 124.7, 124.5, 124.2, 124.1, 123.9, 54.7, 54.6, 54.2, 53.3, 48., 48.0, 43.8, 42.97, 42.91, 34.0, 33.9, 33.8, 17.0, 16.5, 15.9.

DOSY Nuclear Magnetic Resonance (NMR) Experiments. The samples were prepared in deuterium oxide at a concentration between 0.5 and 2 mM (within the infinite

dilution range for similar samples at 0.1–2.1 mM).[37] The experiments have been performed on a The Bruker Ascend™ 400 MHz spectrometer, equipped with a 5 mm BBFO^{PLUS} probe with ^{2}H "lock" channel and *Z* gradient. The spectrometer is also equipped with a control temperature unit prepared to work at temperatures ranging from 0 °C to +50 °C. Gradient strength was calibrated by measuring the diffusion rate of pure water of residual protons in D_2O. All experiments were conducted at 300 K. The samples were allowed to equilibrate for no fewer than 15 min. To determine the diffusion rates, a 2D sequence using double stimulated echo for convection compensation and LED using bipolar gradient pulses for diffusion was used. The Diffusion coefficients (*D*) were determined from the slope of the Stejskal-Tanner plot, which relates it to the signal intensity through the equation: $\ln(\frac{I}{I_0}) = -\gamma^2\delta^2G^2(\Delta - \frac{\delta}{3})D$, where I is the integral of the peak area at a given value of *G*, I_o is the integral of the peak area at a *G*=0, *G* is the gradient field strength, γ is the gyromagnetic ratio, δ is the gradient duration and Δ is the time between the gradient pulses.[36] The diffusion coefficients determined were used to calculate the hydrodynamic radius via the Stokes-Einstein equation: $R_h = K_BT/6\pi\eta D$, where K_B is the Boltzmann constant, T is the temperature and η is the viscosity of the solution (1.0963 cP for D_2O viscosity).[37]

Molecular Dynamics Simulations. Briefly, we utilized the AMBER12 MD software package,[42] with the force field parameters (parm99). For the 1,4-substituted triazole-based dendrimers we used the parameter described before,[43] and those not included were transferred from the General Atom Force Field parameters (GAFF).[44] The initial dendrimer conformations were generated with the Dendrimer Building Tool (DBT)[45] or with AmberTools12 and the LEaP package. The system was minimized and then heated to 300 K over 40 ps. Simulations were run at physiological pH (7.4) in NPT ensemble at 300 K and 1 atm for 20 ns. The cutoff for non-bonded interactions was 9 Å. Time steps of 2 fs were taken with implementation of the SHAKE routine.[46] Dendrimers were equilibrated for 2 ns and starting from these configurations, production runs of 20 ns trajectories were performed under an NPT ensemble. Trajectory analyses were performed using the Amber modules *ptraj* and *cpptraj*. Snapshots from the trajectories within this paper were created with VMD software.[47] Further details of the Molecular Dynamics Simulations are described in the Electronic Supporting Information (ESI).

Luminescent Microscopy experiments with *E. coli* bacteria incubated with $\mathbf{G3_{Naph}NH_2}$. Bacteria were grown in 10 mL of LB Broth at 37ºC in a rocking incubator (18 hours). Then, culture contents were split into four 15 mL vials, centrifuged (5000g, 5 minutes), and washed again in 5 mL PBS. After an additional centrifugation (5000 g, 5 minutes), bacterial pellets were either resuspended in 3 mL PBS with $\mathbf{G3_{Naph}NH_2}$ (10^{-4} M or $5{\cdot}10^{-4}$ M dilution) or resuspended in 3 mL PBS alone. A 8 h incubation step in a rocking incubator followed (4ºC). Then, both samples were centrifuged (5000 g, 5 minutes) and washed twice in 3 mL PBS. Finally, each bacterial sample was resuspended in 100 µL PBS. Bacterial cultures were analyzed using a Leica SP5 MP confocal microscope equipped with Spectraphysics MaiTai HP pulse IR laser for multiphoton excitation and a HCX PL APO lambda blue 63x NA 1.40 oil immersion objective lens was used. Brightfield and confocal images were acquired using 405 nm excitation with emissions detected with a spectral PMT detector set to 500-600 nm. Multiphoton images were acquired sequentially with excitation at 720 nm and detection between 500-550 nm with an external HyD non-descanned detector.

Bactericidal test. To examine the bactericidal effect of $\mathbf{G3_{Naph}NH_2}$ on *E. coli*, approximately $4{\cdot}10^6$ colony-forming units (CFU) were cultured on LB agar plates supplemented with 10 or 100 µM $\mathbf{G3_{Naph}NH_2}$. LB plates cultured ($\mathbf{G3_{Naph}NH_2}$ free) under the same conditions were used as controls. The plates were incubated for 24 h at 37ºC and the number of colonies was recorded. Counts on the three plates corresponding to a particular sample were averaged. To examine the bacterial growth rate as well as to determine the growth curve in the presence of $\mathbf{G3_{Naph}NH_2}$, *E. coli* were grown in liquid LB medium supplemented with 10 or 100 µM. Growth rates and bacterial concentrations were determined by measuring optical density (OD) at 600 nm each 1 hour (OD of 0.1 corresponds to a concentration of 10^8 cells per cm^3) in a FLUOstar Omega de BMG Labtech device.

ASSOCIATED CONTENT

^{1}H, ^{13}C and HSQC spectra of all described compounds, DOSY NMR experiments, IR spectra and Theoretical Calculations. This material is available free of charge via the Internet at http://pubs.acs.org.

AUTHOR INFORMATION

Corresponding Author

*yolvida@uma.es, *inestrosa@uma.es, Tel.: +34-952137565

Author Contributions

The manuscript was written through contributions of all authors. All authors have given approval to the final version of the manuscript. E. Perez-Inestrosa and Y. Vida conceived and designed the experiments; N. Molina performed the chemical synthesis and analysis of the compounds helped by J. A. Guadix and J. M. Perez-Pomares. F. Najera performed molecular dynamic simulation studies.

Funding Sources

This work was supported by the Spanish Ministerio de Economía, Industria y Competitividad (CTQ2016-75870-P), Instituto de Salud Carlos III (ISCIII; RETIC ARADYAL RD16/0006/0012), Consejería de Salud, Junta de Andalucía (PI0250-2016) and FEDER founds. N.M. holds a FPU grant of MECD (FPU15/00641). J.A.G. acknowledges financial support from Plan Propio-Universidad de Málaga.

ACKNOWLEDGMENT

We gratefully acknowledge the computer resources provided by the SCBI (Supercomputing and Bioinformatics Center) of the University of Malaga. We are indebted to Dr. Luis Díaz-

Martínez and Dr. Diego Romero from Departamento de Microbiología, Facultad de Ciencias, Universidad de Málaga (Spain) for their excellent technical assistance and help with the bacterial assays.

ABBREVIATIONS

Boc, *t*Butoxycarbonyl; MALDI-TOF matrix-assisted laser desorption ionization-time of flight.

REFERENCES

(1) Mintzer, M. A.; Grinstaff, M. W.; Paetsch, I.; Hunold, P.; Mahler, M.; Shamsi, K.; Nagel, E.; Price, C. F.; Clark, L. J.; Paull, J. R. A.; et al. Biomedical Applications of Dendrimers: A Tutorial. *Chem. Soc. Rev.* **2011**, *40* (1), 173–190. https://doi.org/10.1039/B901839P.

(2) Naylor, A. M.; Goddard, W. A.; Kiefer, G. E.; Tomalia, D. A. Starburst Dendrimers. 5. Molecular Shape Control. *J. Am. Chem. Soc.* **1989**, *111* (6), 2339–2341. https://doi.org/10.1021/ja00188a079.

(3) Percec, V.; Cho, W. D.; Mosier, P. E.; Ungar, G.; Yeardley, D. J. P. Structural Analysis of Cylindrical and Spherical Supramolecular Dendrimers Quantifies the Concept of Monodendron Shape Control by Generation Number. *J. Am. Chem. Soc.* **1998**, *120* (43), 11061–11070. https://doi.org/10.1021/ja9819007.

(4) Fréchet, J. M. J.; Tomalia, D. A. *Dendrimers and Other Dendritic Polymers*; Wiley, Hoboken, NJ, USA, 2001. https://doi.org/10.1002/0470845821.

(5) Maiti, P. K.; Çağin, T.; Wang, G.; Goddard, W. A. Structure of PAMAM Dendrimers: Generations 1 through 11. *Macromolecules* **2004**, *37* (16), 6236–6254. https://doi.org/10.1021/ma035629b.

(6) Sánchez-Sancho, F.; Pérez-Inestrosa, E.; Suau, R.; Mayorga, C.; Torres, M. J.; Blanca, M.; María J. Torres, A.; Blanca§, M. Dendrimers as Carrier Protein Mimetics for IgE Antibody Recognition. Synthesis and Characterization of Densely Penicilloylated Dendrimers. *Bioconjug. Chem.* **2002**, *13* (3), 647–653. https://doi.org/10.1021/BC0155824.

(7) Montañez, M. I.; Najera, F.; Mayorga, C.; Ruiz-Sanchez, A. J.; Vida, Y.; Collado, D.; Blanca, M.; Torres, M. J.; Perez-Inestrosa, E. Recognition of Multiepitope Dendrimeric Antigens by Human Immunoglobulin E. *Nanomedicine Nanotechnology, Biol. Med.* **2015**, *11* (3), 579–588. https://doi.org/10.1016/j.nano.2015.01.006.

(8) Mayorga, C.; Perez-Inestrosa, E.; Molina, N.; Montañez, M. I. Development of Nanostructures in the Diagnosis of Drug Hypersensitivity Reactions. *Curr. Opin. Allergy Clin. Immunol.* **2016**, *16* (4), 300–307. https://doi.org/10.1097/ACI.0000000000000282.

(9) Buhleier, E.; Wehner, W.; Vögtle, F. "Cascade"- and "Nonskid-Chain-like" Syntheses of Molecular Cavity Topologies. *Synthesis (Stuttg).* **1978**, *1978* (02), 155–158. https://doi.org/10.1055/s-1978-24702.

(10) Denkewalter, R. G.; Kolc, J. F.; Lukasavage, W. J.; Stroup, K. E.; Stewart, R. C.; Doernberg, A. M. Macromolecular Highly Branched Homogeneous Compound. United States Patent, 4,410,688, 1983.

(11) Tomalia, D. A.; Baker, H.; Dewald, J.; Hall, M.; Kallos, G.; Martin, S.; Roeck, J.; Ryder, J.; Smith, P. A New Class of Polymers: Starburst-Dendritic Macromolecules. *Polym. J.* **1985**, *17* (1), 117–132. https://doi.org/10.1295/polymj.17.117.

(12) Tomalia, D. A.; Naylor, A. M.; Goddard, W. A. Starburst Dendrimers: Molecular-Level Control of Size, Shape, Surface Chemistry, Topology, and Flexibility from Atoms to Macroscopic Matter. *Angew. Chemie Int. Ed. English* **1990**, *29* (2), 138–175. https://doi.org/10.1002/anie.199001381.

(13) Stenström, P.; Hjorth, E.; Zhang, Y.; Andrén, O. C. J.; Guette-Marquet, S.; Schultzberg, M.; Malkoch, M. Synthesis and in Vitro Evaluation of Monodisperse Amino-Functional Polyester Dendrimers with Rapid Degradability and Antibacterial Properties. *Biomacromolecules* **2017**, *18* (12), 4323–4330. https://doi.org/10.1021/acs.biomac.7b01364.

(14) Falkovich, S.; Markelov, D.; Neelov, I.; Darinskii, A. Are Structural Properties of Dendrimers Sensitive to the Symmetry of Branching? Computer Simulation of Lysine Dendrimers. *J. Chem. Phys.* **2013**, *139* (6), 064903. https://doi.org/10.1063/1.4817337.

(15) Lloyd, J. R.; Jayasekara, P. S.; Jacobson, K. A. Characterization of Polyamidoamino (PAMAM) Dendrimers Using in-Line Reversed Phase LC Electrospray Ionization Mass Spectrometry. *Anal. Methods* **2016**, *8* (2), 263–269. https://doi.org/10.1039/C5AY01995H.

(16) Ruiz-Sanchez, A. J.; Mesa-Antunez, P.; Barbero, N.; Collado, D.; Vida, Y.; Najera, F.; Perez-Inestrosa, E. Synthesis of All-Aliphatic Polyamide Dendrimers Based on a 3,3′-Diaminopivalic Acid Scaffold. *Polym. Chem.* **2015**, *6* (16), 3031–3038. https://doi.org/10.1039/C5PY00154D.

(17) Soler, M.; Mesa-Antunez, P.; Estevez, M.-C.; Ruiz-Sanchez, A. J.; Otte, M. A.; Sepulveda, B.; Collado, D.; Mayorga, C.; Torres, M. J.; Perez-Inestrosa, E.; et al. Highly Sensitive Dendrimer-Based Nanoplasmonic Biosensor for Drug Allergy Diagnosis. *Biosens. Bioelectron.* **2015**, *66*, 115–123. https://doi.org/10.1016/j.bios.2014.10.081.

(18) Mesa-Antunez, P.; Collado, D.; Vida, Y.; Najera, F.; Fernandez, T.; Torres, M.; Perez-Inestrosa, E. Fluorescent BAPAD Dendrimeric Antigens Are Efficiently Internalized by Human Dendritic Cells. *Polymers (Basel).* **2016**, *8* (4), 111. https://doi.org/10.3390/polym8040111.

(19) Jishkariani, D.; MacDermaid, C. M.; Timsina, Y. N.; Grama, S.; Gillani, S. S.; Divar, M.; Yadavalli, S. S.; Moussodia, R.-O.; Leowanawat, P.; Berrios Camacho, A. M.; et al. Self-Interrupted Synthesis of Sterically Hindered Aliphatic Polyamide Dendrimers. *Proc. Natl. Acad. Sci. U. S. A.* **2017**, *114* (12), E2275–E2284. https://doi.org/10.1073/pnas.1700922114.

(20) Hawker, C. J.; Frechet, J. M. J. Preparation of Polymers with Controlled Molecular Architecture. A New Convergent Approach to Dendritic Macromolecules. *J. Am. Chem. Soc.* **1990**, *112* (21), 7638–7647. https://doi.org/10.1021/ja00177a027.

(21) Grayson, S. M.; Fréchet, J. M. J. Convergent Dendrons and Dendrimers: From Synthesis to Applications. *Chemical Reviews*. American Chemical Society 2001, pp 3819–3867. https://doi.org/10.1021/cr990116h.

(22) Wu, P.; Feldman, A. K.; Nugent, A. K.; Hawker, C. J.; Scheel, A.; Voit, B.; Pyun, J.; Fréchet, J. M. J. J.; Sharpless, K. B.; Fokin, V. V. Efficiency and Fidelity in a Click-Chemistry Route to Triazole Dendrimers by the Copper(I)-Catalyzed Ligation of Azides and Alkynes. *Angew. Chemie - Int. Ed.* **2004**, *43* (30), 3928–3932. https://doi.org/10.1002/anie.200454078.

(23) Rostovtsev, V. V.; Green, L. G.; Fokin, V. V.; Sharpless, K. B. A Stepwise Huisgen Cycloaddition Process: Copper(I)-Catalyzed Regioselective "Ligation" of Azides and Terminal Alkynes. *Angew. Chemie Int. Ed.* **2002**, *41* (14), 2596–2599. https://doi.org/10.1002/1521-3773(20020715)41:14<2596::AID-ANIE2596>3.0.CO;2-4.

(24) Carlmark, A.; Hawker, C.; Hult, A.; Malkoch, M. New Methodologies in the Construction of Dendritic Materials. *Chem. Soc. Rev.* **2009**, *38* (2), 352–362. https://doi.org/10.1039/B711745K.

(25) Walter, M. V.; Malkoch, M.; Soderlind, E.; Ohshimizu, K.; Hunt, J. N.; Sivanandan, K.; Montanez, M. I.; Malkoch, M.; Ueda, M.; Hawker, C. J.; et al. Simplifying the Synthesis of Dendrimers: Accelerated Approaches. *Chem. Soc. Rev.* **2012**, *41* (13), 4593. https://doi.org/10.1039/c2cs35062a.

(26) Franc, G.; Kakkar, A. K. "Click" Methodologies: Efficient, Simple and Greener Routes to Design Dendrimers. *Chem. Soc. Rev.* **2010**, *39* (5), 1536. https://doi.org/10.1039/b913281n.

(27) Arseneault, M.; Wafer, C.; Morin, J. F. Recent Advances in Click Chemistry Applied to Dendrimer Synthesis. *Molecules*.

Multidisciplinary Digital Publishing Institute May 20, 2015, pp 9263–9294. https://doi.org/10.3390/molecules20059263.

(28) Blumenstein, J. J.; Michejda, C. J. Bistriazenes: Multifunctional Alkylating Agents. *Tetrahedron Lett.* **1991**, *32* (2), 183–186. https://doi.org/10.1016/0040-4039(91)80849-2.

(29) Delavaux-Nicot, A. C. C. T. R. L. A. O. B. *Dendrimers: Towards Catalytic, Material and Biomedical Uses*; Caminade, A.-M., Turrin, C.-O., Laurent, R., Ouali, A., Delavaux-Nicot, B., Eds.; Chichester, UK, 2011. https://doi.org/10.1002/9781119976530.

(30) Mancuso, L.; Knobloch, T.; Buchholz, J.; Hartwig, J.; Möller, L.; Seidel, K.; Collisi, W.; Sasse, F.; Kirschning, A. Preparation of Thermocleavable Conjugates Based on Ansamitocin and Superparamagnetic Nanostructured Particles by a Chemobiosynthetic Approach. *Chem. - A Eur. J.* **2014**, *20* (52), 17541–17551. https://doi.org/10.1002/chem.201404502.

(31) Amaral, S. P.; Tawara, M. H.; Fernandez-Villamarin, M.; Borrajo, E.; Martínez-Costas, J.; Vidal, A.; Riguera, R.; Fernandez-Megia, E. Tuning the Size of Nanoassembles: A Hierarchical Transfer of Information from Dendrimers to Polyion Complexes. *Angew. Chemie Int. Ed.* **2018**, *57* (19), 5273–5277. https://doi.org/10.1002/anie.201712244.

(32) Lee, J. W.; Kim, H. J.; Han, S. C.; Kim, J. H.; Jin, S.-H. Designing Poly(Amido Amine) Dendrimers Containing Core Diversities by Click Chemistry of the Propargyl Focal Point Poly(Amido Amine) Dendrons. *J. Polym. Sci. Part A Polym. Chem.* **2008**, *46* (3), 1083–1097. https://doi.org/10.1002/pola.22451.

(33) Zhang, C.; Tomalia, D. A. Gel Electrophoretic Characterization of Dendritic Polymers. In *Dendrimers and Other Dendritic Polymers*; John Wiley & Sons, Ltd: Chichester, UK, 2003; pp 237–253. https://doi.org/10.1002/0470845821.ch10.

(34) Xiao, T.; Cao, X.; Wang, S.; Shi, X. Probing the Molecular Weight of Poly(Amidoamine) Dendrimers and Derivatives Using SDS-PAGE. *Anal. Methods* **2011**, *3* (10), 2348. https://doi.org/10.1039/c1ay05361b.

(35) Fritzinger, B.; Scheler, U. Scaling Behaviour of PAMAM Dendrimers Determined by Diffusion NMR. *Macromol. Chem. Phys.* **2005**, *206* (13), 1288–1291. https://doi.org/10.1002/macp.200500048.

(36) van Dongen, M. A.; Orr, B. G.; Banaszak Holl, M. M. Diffusion NMR Study of Generation-Five PAMAM Dendrimer Materials. *J. Phys. Chem. B* **2014**, *118* (25), 7195–7202. https://doi.org/10.1021/jp504059p.

(37) Jiménez, V. A.; Gavín, J. A.; Alderete, J. B. Scaling Trend in Diffusion Coefficients of Low Generation Go–G3 PAMAM Dendrimers in Aqueous Solution at High and Neutral PH. *Struct. Chem.* **2012**, *23* (1), 123–128. https://doi.org/10.1007/s11224-011-9844-6.

(38) Gupta, S.; Biswas, P. Effect of PH on Size and Internal Structure of Poly(Propylene Imine) Dendrimers: A Molecular Dynamics Simulation Study. *J. Phys. Chem. B* **2018**, *122* (39), 9250–9263. https://doi.org/10.1021/acs.jpcb.8b04653.

(39) Collado, D.; Remón, P.; Vida, Y.; Najera, F.; Sen, P.; Pischel, U.; Perez-Inestrosa, E. Energy Transfer in Aminonaphthalimide-Boron-Dipyrromethene (BODIPY) Dyads upon One- and Two-Photon Excitation: Applications for Cellular Imaging. *Chem. Asian J.* **2014**, *9* (3), 797–804. https://doi.org/10.1002/asia.201301334.

(40) Strassert, C. A.; Otter, M.; Albuquerque, R. Q.; Höne, A.; Vida, Y.; Maier, B.; De Cola, L. Photoactive Hybrid Nanomaterial for Targeting, Labeling, and Killing Antibiotic-Resistant Bacteria. *Angew. Chemie Int. Ed.* **2009**, *48* (42), 7928–7931. https://doi.org/10.1002/anie.200902837.

(41) Levenson, R. M.; Lynch, D. T.; Kobayashi, H.; Backer, J. M.; Backer, M. V. Multiplexing with Multispectral Imaging: From Mice to Microscopy. *ILAR J.* **2008**, *49* (1), 78–88. https://doi.org/10.1093/ilar.49.1.78.

(42) D. A. Case, T. A. Darden, T. E. Cheatham, III, C. L. Simmerling, J. Wang, R. E. Duke, R. Luo, R. C. Walker, W. Zhang, K. M. Merz, B. P. Roberts, S. Hayik, A. E. Roitberg, G. Seabra, J. M. Swails, I. Kolossváry, K. F. Wong, F. Paesani, J. Vanicek, R. M. Wo, A. K. and P. A. K. AMBER 12, University of California, San Francisco. 2012.

(43) Marion, A.; Góra, J.; Kracker, O.; Fröhr, T.; Latajka, R.; Sewald, N.; Antes, I. Amber-Compatible Parametrization Procedure for Peptide-like Compounds: Application to 1,4- and 1,5-Substituted Triazole-Based Peptidomimetics. *J. Chem. Inf. Model.* **2018**, *58* (1), 90–110. https://doi.org/10.1021/acs.jcim.7b00305.

(44) Wang, J.; Wolf, R. M.; Caldwell, J. W.; Kollman, P. A.; Case, D. A. Development and Testing of a General Amber Force Field. *J. Comput. Chem.* **2004**, *25* (9), 1157–1174. https://doi.org/10.1002/jcc.20035.

(45) Maingi, V.; Jain, V.; Bharatam, P. V.; Maiti, P. K. Dendrimer Building Toolkit: Model Building and Characterization of Various Dendrimer Architectures. *J. Comput. Chem.* **2012**, *33* (25), 1997–2011. https://doi.org/10.1002/jcc.23031.

(46) Ryckaert, J.-P.; Ciccotti, G.; Berendsen, H. J. . Numerical Integration of the Cartesian Equations of Motion of a System with Constraints: Molecular Dynamics of n-Alkanes. *J. Comput. Phys.* **1977**, *23* (3), 327–341. https://doi.org/10.1016/0021-9991(77)90098-5.

(47) Humphrey, W.; Dalke, A.; Schulten, K. VMD: Visual Molecular Dynamics. *J. Mol. Graph.* **1996**, *14* (1), 33–38. https://doi.org/10.1016/0263-7855(96)00018-5.

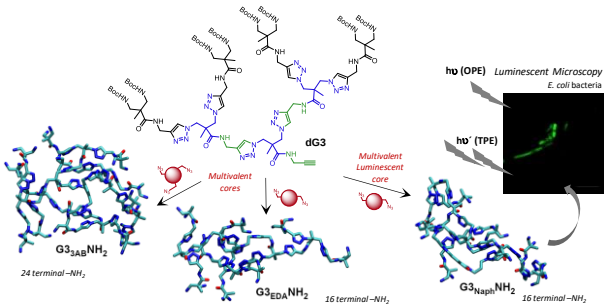
dG3
Multivalent cores
Multivalent Luminescent core
hυ (OPE)
Luminescent Microscopy
E. coli bacteria
hυ' (TPE)
G3AABNH2
24 terminal –NH2
G3EDANH2
16 terminal –NH2
G3NaphNH2
16 terminal –NH2